DOE/ER/12082-1

DOE/ER/12082-1
DISTRIBUTION CATEGORY- UC

INVESTIGATION OF MAGMA CHAMBERS IN THE WESTERN GREAT BASIN

FINAL REPORT
FOR THE PERIOD

9 June 1982 to 31 October 1985

William A. Peppin
10 February 1986

Seismological Laboratory
Mackay School of Mines
University of Nevada-Reno
Reno, Nevada 89557

PREPARED FOR THE

U.S. DEPARTMENT OF ENERGY
OFFICE OF ENERGY RESEARCH
DIVISION OF ENGINEERING, MATHEMATICS & GEOSCIENCES

LEGIBILITY NOTICE

A major purpose of the Technical Information Center is to provide the broadest dissemination possible of information contained in DOE's Research and Development Reports to business, industry, the academic community, and federal, state and local governments.

Although a small portion of this report is not reproducible, it is being made available to expedite the availability of information on the research discussed herein.

TABLE OF CONTENTS

INVESTIGATION OF MAGMA CHAMBERS IN THE WESTERN GREAT BASIN

DOE Contract DE-AS08-82ER12082

June 9, 1982 to October 31, 1985

Introduction.

This document is the final report to the Department of Energy from the University of Nevada Seismological Laboratory covering work done under the above-named contract. It covers investigations undertaken in the western Great Basin with emphasis on the Mammoth Lakes, California region.

Work by personnel at the University of Nevada Seismological Laboratory has contributed significantly to the delineation of shallow crustal attenuating bodies in and south of Long Valley caldera (Ryall and Ryall, 1981, 1983; Sanders and Ryall, 1983; Sanders, 1984; Ryall and Ryall, 1984). In connection with the Mammoth Lakes earthquake sequence that started in 1978, they noted that shallow earthquakes occurring near the southern boundary of the caldera produced earthquakes with P-waves depleted in high-frequency content and no S-waves at all at regional stations to the north. This work led to the suggestion by Sanders and Ryall (1983) that several magma chambers were present in the caldera at depths of 4 to 8 km. Further studies of S-wave shadowing led Ryall and Ryall (1984) to propose a crustal anomaly, possibly associated with magma, near the south end of the Hilton Creek fault, 10 km south of the caldera.

Magma has almost certainly been recently intruded to shallow depths in Long Valley caldera, as is most clearly evidenced by recent uplift of the resurgent dome within the caldera (Savage and Clark, 1982; Rundle and Whitcomb, 1984). The presence of recently-intruded magma *south* of the caldera would open the possibility of a system of feeder dikes connecting these two magma bodies and provide fundamental information about the timing and physics of this process (e.g., the possibility that intrusion of magma, like the seismicity, first occurred 10 km south of the caldera). One clear advantage of working with a possible magma zone south of the caldera is that the sites over this zone, being mostly on hard rock, provide a potentially clearer view down into the associated earthquake source zone than stations located in the caldera. Under our just completed DOE contract, we have expanded our seismic network to provide better coverage of this southern seismic zone. Our plan was to place seismometers directly over the earthquakes occurring in the Sierran mountain block to provide well-controlled hypocentral information on these sources, and to place stations along the west flank of the White Mountains to observe raypaths that would pass through suspected attenuating bodies. As often happens in science, the natural phenomena did not conform to the plan. Instead, seismicity in the mountain block became progressively more quiescent during Fall 1984. Subsequently, the November 1984 Round Valley earthquake occurred east of the mountain block in the center of the dense array of stations, with especially good azimuthal control provided by the White Mountains stations. This magnitude 6 event produced thousands of recorded aftershocks, some of which showed

anomalous phases at the stations placed in the Sierra Nevada. These data have provided more evidence on the nature of the possible magma intrusion at the south end of Hilton Creek fault. The arrival times and wave character of these anomalous seismic phases have led us to suppose that they are P reflections, much like those found by Hill (1976) in the NW part of the caldera. These phases are so strong and are seen so frequently that we are now able to hypothesize the approximate geometry of a causative body (roughly cylindrical, four to eight km deep, and perhaps 2 km wide). This report provides some of the latest information covering our efforts in this area.

This report summarizes our work on three basic tasks: (1) network operations, (2) data analysis and interpretation, and (3) study of magma bodies. We conclude the report with a summary of abstracts and publications which have been supported by this contract. Numbered

Task 1. Network Operations.

All research done under this contract draws from seismic data taken from the UNR-USGS-DOE seismic array. Operation of this network is therefore playing a vital role in providing detailed monitoring of an area of known geothermal resources, and with potential for both major volcanic eruptions and tectonic earthquakes. This section describes network operations during the recent contracting period.

Current Network

The University of Nevada is currently operating 56 seismic stations in western Nevada and eastern California, with heavy emphasis on the Long Valley region. In addition to our own stations, we also receive telemetered signals from stations operated by other agencies, 2 from the University of California, 1 from the California Department of Water Resources, and 15 from the USGS at Menlo Park. Our current 74-station network is listed in **Table 1**, and the Long Valley area stations are shown in **Figure 1**. Including multi-components and time signals, we are currently recording 88 channels of data from this network.

Data Acquisition and Analysis

Analog System. Since 1969, all signals from the telemetered network have been recorded on analog magnetic tape. Simultaneously, eight selected stations are monitored on Helicorder paper-drum recorders. Until recently the Helicorders were scanned to choose events for detailed analysis, and those events were played out on 16-channel strip-chart (Siemens ink-jet) recordings using switch-selectable groups of stations. The Siemens records were timed by hand, cards were punched from the reading sheets, and the data were fed into the PDP-11/70 for hypocenter and magnitude determination. The analog-tape recording system is still functional, and is preserved today as a backup system.

On-line System. A computer-based earthquake recording system has been operating at UNR since May 1984 and is triggering successfully on local events, regional earthquakes, teleseisms, and explosions. It provides on-line event detection and digitization of the analog seismic signals transmitted to the Reno data facility. This system facilitates analysis of large numbers of earthquakes and will allow waveform analysis of the network data. The triggering algorithm has been tuned sufficiently that false triggers comprise 10% of the total number of events recorded. We are currently recording 84 seismic signals and 4 time signals on the 96-channel on-line system. The data are processed with an

TABLE 1.

Stations recorded by UNR on 7/1/85

code	station	latitude	longitude	elev	stat #	agn	comp	instr
BAB	Babbitt Peak	39 36.08	120 6.24	2664	8211	UNR	SP Z	S-13
BCK	Birch Creek	37 41.85	118 22.32	1634	840913	UNR	SP Z	HS-10
BEN	Benton	37 42.93	118 34.40	2490	831020	UNR	SP Z	HS-10
BFC	Buffalo Canyon	38 53.64	119 36.46	1743	7802	UNR	SP Z	L-4
BHP	Bishop	37 17.97	118 29.24	2171	640810	UNR	SP Z	HS-10
BIS	Bismarck Peak	39 7.43	119 40.50	1786	7803	UNR	SP Z	L-4
BMT	Battle Mountain	40 25.68	117 13.30	1500	690902	UNR	WB 3	SL-210,220
BMR	Black Mountain	40 6.52	120 17.46	2146	780518	UNR	SP Z	L-4
BQN	Boundary Peak	37 57.31	118 18.10	2562	7407	UNR	SP Z	L-4
CAS	Casa Diablo Mtn	37 34.49	118 33.09	2170	821105	UNR	SP Z	HS-10
CDS	Casa Diablo Hot Spr	37 39.30	118 54.25	2384	820803	USGS	SP Z	L-4
CLK	Crowley Lake	37 35.44	118 49.45	2576	7911	USGS	SP Z	L-4 installed by UNR
CHC	Coldwater Canyon	37 29.69	118 18.38	2000	640810	UNR	SP Z	HS-10
DIX	Dixie Hot Springs	39 48.13	118 4.92	1143	8001	UNR	SP Z	L-4
DLH	Downhole	37 42.94	118 55.76	2232	850109	UNR	SP 3	L-4-3DS
DMP	Dunphy Pass	37 42.48	119 2.75	2550	640216	USGS	SP Z	L-4
DOE	Doe Ridge	37 38.25	118 50.00	1700	831109	USGS	SP Z	L-4
DSX	Dixie Settlement	39 42.57	118 03.72	1037	850214	UNR	SP Z	HS-10
EBP	Ebbets Pass	38 35.00	119 48.22	2432	801216	UNR	SP Z	L-4
EMB	Emerald Bay	38 58.48	120 06.16	2122	841101	UNR	SP Z	HS-10
FER	Five Bridges	37 25.77	118 25.70	1366	850523	USGS	SP Z	L-4
FLV	Fish Lake Valley	37 49.84	117 54.57	1689	831018	UNR	SP Z	HS-10
FPK	Fairview Peak	39 12.32	118 9.26	2256	710930	UNR	SP Z	Benioff
FRI	Friant	36 59.5	119 42.5	119	840720	UCB	SP Z	Benioff
GBK	Glenbrook	39 05.77	119 55.22	2268	841012	UNR	SP Z	S-13
GMO	Genoa	38 55.75	119 51.17	1646	7802	UNR	SP Z	L-4
GRP	Gravel Pit	37 37.59	118 54.08	2208	850523	USGS	SP Z	L-4
GVR	Gabbs Valley Range	38 39.44	118 9.58	2550	831016	UNR	SP Z	HS-10
HCK	Hamtoon Creek	38 4.53	118 35.53	1690	800926	UNR	SP Z	L-4
HDP	Hopkins Lake	37 26.98	118 49.76	3220	840718	UNR	SP Z	L-4
HTC	Hilton Creek	37 31.79	118 46.26	3012	840719	UNR	SP Z	HS-10
HYX	Hoyt Mine	39 46.37	117 45.80	1661	811111	UNR	SP Z	S-13
IND	Independence	39 26.06	120 17.50	2146	7711	UNR	SP Z	S-13
JAS	Jamestown	37 56.80	120 26.30	457	691020	UCB	SP Z	Benioff
KBF	Kyburz Flat	39 30.41	120 12.71	2079	7306	UNR	SP Z	S-13
KVN	Kaiserville	39 3.06	118 6.00	1629	720113	UNR	SP Z	Benioff
LCC	Laurel Creek Canyon	37 36.65	118 54.92	2511	820803	USGS	SP Z	L-4
LHV	Little Hamtoon Vly	38 15.07	118 30.27	2225	800926	UNR	SP Z	L-4
LLK	Laurel Lakes	37 34.73	118 54.30	3030	8310	USGS	SP Z	L-4
LMC	Lookout Mountain	37 43.70	118 56.71	2520	7911	USGS	SP Z	L-4 installed by UNR
LOY	Loyalton	39 39.52	120 14.15	1582	8211	UNR	SP Z	S-13
LUL	Lundy Lake	38 3.14	119 10.62	2243	810417	UNR	SP Z	L-4
MCC	Mono Craters	37 55.17	119 1.46		830728	UNR	SP Z	HS-10
MDP	Devil's Postpile	37 37.94	119 4.74		850523	USGS	SP 3	L-4
MGC	McGee Creek	37 32.70	118 49.07	2561	840809	UNR	SP Z	L-4
MGN	McGee Canyon	37 48.80	118 41.73	2522	801121	UNR	SP Z	L-4
MLK	Mammoth Lakes	37 39.86	118 58.53	2671	820803	USGS	SP Z	L-4
MLN	Millner Creek	37 35.63	118 20.56	1780	840913	UNR	SP Z	HS-10
MMC	Masonic Mountain	38 21.65	119 7.70	2548	801121	UNR	SP Z	L-4
MMP	Mammoth Pass	37 36.60	119 1.68	2870	640216	USGS	SP Z	L-4
MNA	Mina	38 25.97	118 9.40	1524	8303	UNR	WB 3	SL-210,220
MNA	Mina (MAN,MIN,MIV)	38 25.97	118 9.40	1524	72	UNR	SP Z	Benioff
MON	Mono Valley	38 3.65	118 46.55	2179	75	UNR	SP Z	L-4
MPK	Martis Peak	39 17.74	120 1.81	2484	7304	UNR	SP Z	L-4
CRC	Owens River	37 38.12	118 39.36	2301	7911	UNR	SP Z	L-4
CRV	Oroville	39 33.34	121 13.00	362	691020	CDWR	SP Z	Benioff
POC	Poleta Canyon	37 21.74	118 16.75	1799	840913	UNR	SP Z	HS-10
POW	Powell Mountain	38 24.67	118 37.91	1890	8010	UNR	SP Z	L-4
PRB	Pioneer Basin	37 28.91	118 48.17	3399	840719	UNR	SP Z,E	L-4
RCC	Rock Creek Canyon	37 29.26	118 43.30	2800	831027	UNR	SP Z	HS-10
RSM	Red Slate Mountain	37 30.55	118 52.68	3685	8307	USGS	SP Z	L-4 repaired by UNR
RYN	Ryan	38 37.69	118 31.38	1585	75	UNR	SP Z	L-4
SCH	Scheelite	37 21.95	118 41.22	2365	810108	UNR	SP Z	L-4
SHL	Sherwin Lakes	37 37.05	118 57.25	2499	820518	USGS	SP Z	L-4
SJC	Sonora Junction	38 20.95	119 26.35	2256	801216	UNR	SP Z	L-4
SLK	Silver Lake	37 50.04	119 7.72		830728	UNR	SP Z	HS-10
STR	Mt. Starr	37 26.20	118 45.60	3704	840719	UNR	SP Z	L-4
TAH	Tahoe City	39 9.00	120 9.78	2097	8306	UNR	SP Z	S-13
TNK	Tinker's Knob	39 16.05	120 14.15	2428	7305	UNR	SP Z	L-4
TNP	Tonopah	38 4.92	117 13.06	1939	631011	UNR	SP 3	Benioff
TUN	Tungsten	37 21.20	118 33.81	1810	850523	USGS	SP Z	L-4
VIP	Virginia Peak	39 45.24	119 27.65	2499	780426	UNR	SP Z	L-4
VPK	Verdi Peak	39 28.48	120 2.24	2469	7307	UNR	SP Z	S-13
WCN	Washoe City	39 18.10	119 45.36	1704	8303	UNR	WB 3	SL-210,220
WMD	Wells Meadows	37 26.61	118 38.22	1683	831027	UNR	SP Z	HS-10

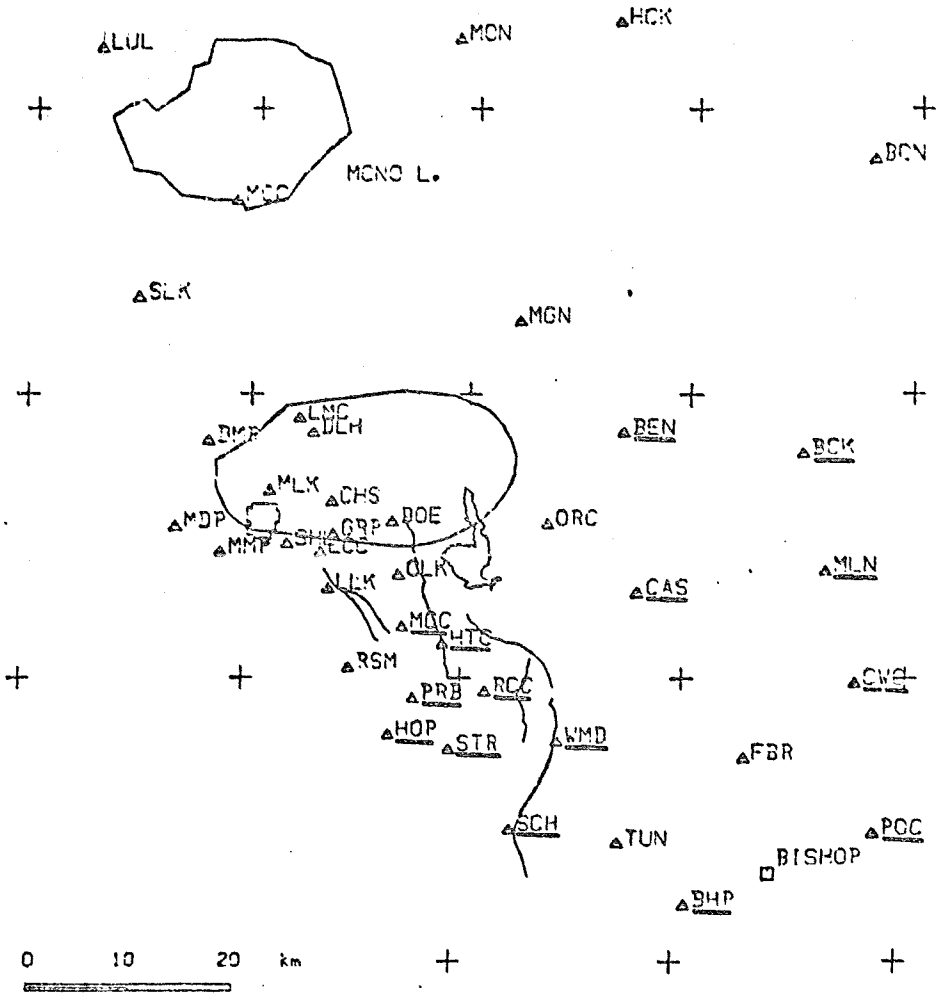

Figure 1. Seismic stations in the Mammoth Lakes region as of 01 July 1985. Stations installed with DOE funding are underlined.

interactive graphics software package developed at the University of Washington that allows rapid timing and location of earthquakes. All arrival time picking is done by human analysts, but the computer system has greatly reduced the errors which are of necessity associated with analog analysis. During the first year of operation we have recorded and archived digital seismograms for 6129 seismic events. Of this number 3544 (58%) are local earthquakes that we have located and cataloged. The remainder of the data are teleseisms, regional events, nuclear tests, and local events of less than 10 seconds duration, (roughly magnitude < 1.5 M_L), for which we save the traces but do not time the arrivals. The Helicorders are still scanned on a daily basis to guarantee that no events are missed, but the experience has been that the on-line system records more events and down to a lower threshold than was previously achieved with the hand-analysis method.

Digital Stations. The University of Nevada has constructed a 4-station, telemetering digital array which is now deployed in mine tunnels at Battle Mountain (BMN), Mina (MNA) Washoe City (WCN) and Donnelly Peak (DNY), and telemeters continuous digital data from those sites to the University recording facility. The stations are designed as a completely digital data acquisition system, featuring 72 dB resolution, 96 dB dynamic range, and 0.05-20 Hz signal bandpass (Nicks, *et al.*, 1983). Data from the stations are phase encoded and input to a 1200-baud modem for VHF radio transmission to the recording facility at Reno. The design uses CMOS technology to reduce power consumption which facilitates battery or solar-powered operation. The recording system consists of a computer input assembly that accepts phase modulated data from the field stations and formats it for input to an LSI-11/23 computer. The data are continuously recorded on digital magnetic tape. Efforts are under way to increase the sampling rate from 25 to 50 samples/sec and to expand the station capacity of the computer. In order to accommodate the increased data rate, the 11/23 will be switched from continuous to event-triggered recording. Four stations are currently in operation, and we expect to add one station per year over the next three years.

Task 2. Analysis and Interpretation

In the course of our work on this contract with the Department of Energy, we have placed major emphasis on the interpretation of basic seismological data as it pertains to the seismotectonics of the Mammoth Lakes region, with emphasis on the possible location of shallow crustal magma. These basic data sets comprise (1) seismicity, (2) focal mechanisms, and (3) waveform analysis. Contributions in each of these areas are described in this section.

2.1 Seismicity

2.1.1 Relocations of the Earlier Earthquakes

Mammoth Lakes events. During this reporting period the work of C. S. Lide appeared in print. The main contribution of this work was to present a set of precise master-event locations of the early part of the aftershock sequence of the 1980 Mammoth Lakes earthquakes. Before discussing the results, we present a commentary on the importance of the master event method as applied in this region.

The so-called *master-event location method* is a procedure for determining quite accurate *relative locations* of hypocenters even if the density of the recording stations is quite low, as it was at the time of the 1980 sequence (UNR was operating only three telemetered stations in the area at the time). The

essence of this method is to choose a well located earthquake and assume that the travel-time residuals observed for it are a reflection of the uncertainities in the velocity model. The residuals are then employed as station corrections to locate other events that are close to the "master event" in space and time. This assumption can introduce a systematic error in that all of the relocated events will be displaced by the distance between the calculated and the "true" location of the master event. However, this method subtracts out the random component of the velocity model errors and usually gives a truer picture of the relative locations of the earthquakes to each other. The master-event technique can be made extremely rigorous by calibrating the master with explosion data and by being highly selective in the choice stations used. Compare, for example, locations computed using ordinary methods of the 1978 Wheeler Crest aftershocks with locations found, using much the same data, via the master-event method, shown in Figure 2. Using the ordinary method, a rather diffuse cloud of earthquakes is given, while the master event method quite clearly shows an north-south lineup of epicenters (Figure 3). Using a dense array of stations placed over the aftershock region, the USGS has located some of these aftershocks (Figure 22). If one believes that earthquakes should line up on linear features, such as faults, a comparison of these figures suggests that the master-event locations are probably correct.

This point is particularly important at Mammoth Lakes, where the stations coverage was sparse during this time period. Preliminary epicenters determined showed a similar tendency toward an amorphous cloud of events. A major question was this: on what structures were these thousands of earthquakes occurring? In the absence of sufficiently precise locations, it was not possible to answer this question, particularly because there seemed to be no correlation between the seismicity and the obvious major Holocene faulting features of the Mammoth Lakes region, such as the Hilton Creek fault. This left researchers in quite a quandary. It was therefore quite important to attempt precise relative locations to see if, in fact, the earthquakes were occurring on structures either known or unknown.

Somerville and Peppin (1980) were the first to report master-event locations of Mammoth Lakes earthquakes. They found that the seismicity above magnitude 4.0 appeared to concentrate on N-S lineaments. However, the work was justly criticized for relying on a small number (only 50) events. Therefore, it was important to try and perform master-event analysis on a larger subset of a complex data set comprising about 10,000 earthquakes. This was one of the contributions made by Lide in his Master's thesis.

Shown in Figure 4 are master-event locations given by Lide (1984), on the right (for comparison, the UNR catalog locations are given on the left, again showing how the master event procedure tends to reduce the scatter of the epicenters computed). The number of events Lide used is limited by a rigorous application of the master-event technique, which required that the same stations be used for all of the events. However, in this figure, as found by Somerville and Peppin (1980), the events tend to show two lineations (NNE rather than N, however). Although this trend is not what one would expect based on the geology of the area, the precision of the locations gives quite unequivocal evidence for such trends, and Lide sought to find an explanation. He noted that Mayo (1937) had done a study of jointing in the Mesozoic rocks of the mountain block south of the caldera, and had shown a strong incidence of NNE jointing in these rocks (Figure 5). This suggests that present earthquakes south of the caldera may be occurring on lines of preexisting weakness (the NNE joints) and therefore that the tectonics giving rise to active volcanism in Quaternary times around the caldera may now be speading south.

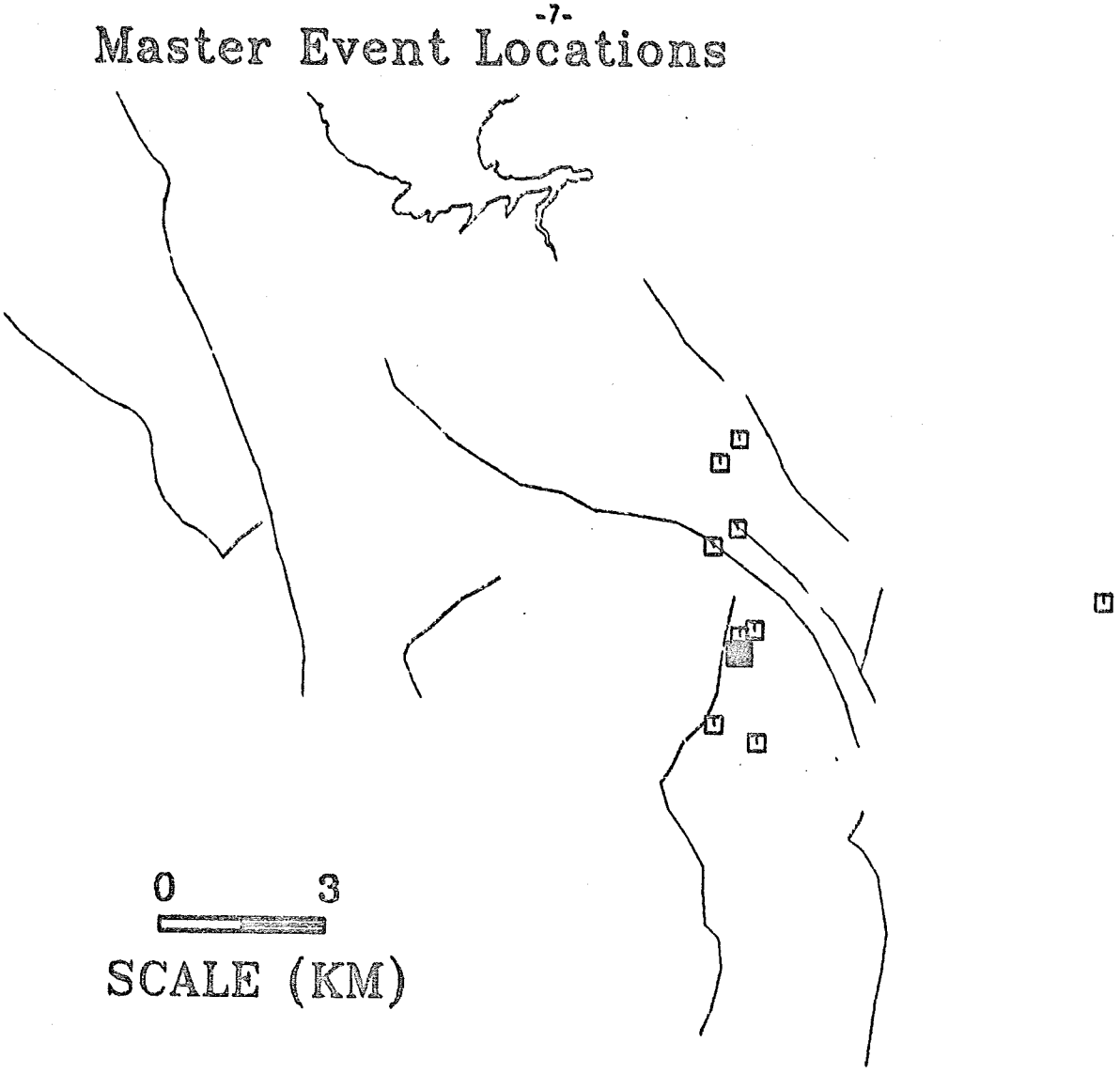

Figure 2. Master-event locations for aftershocks (with magnitude 4 and greater) of the 04 October 1978 Wheeler Crest earthquake (Somerville and Peppin, 1979). Solid square: main shock. Exactly the same stations and station weights were used to perform these locations relative to a master event (which was located using many more and local stations).

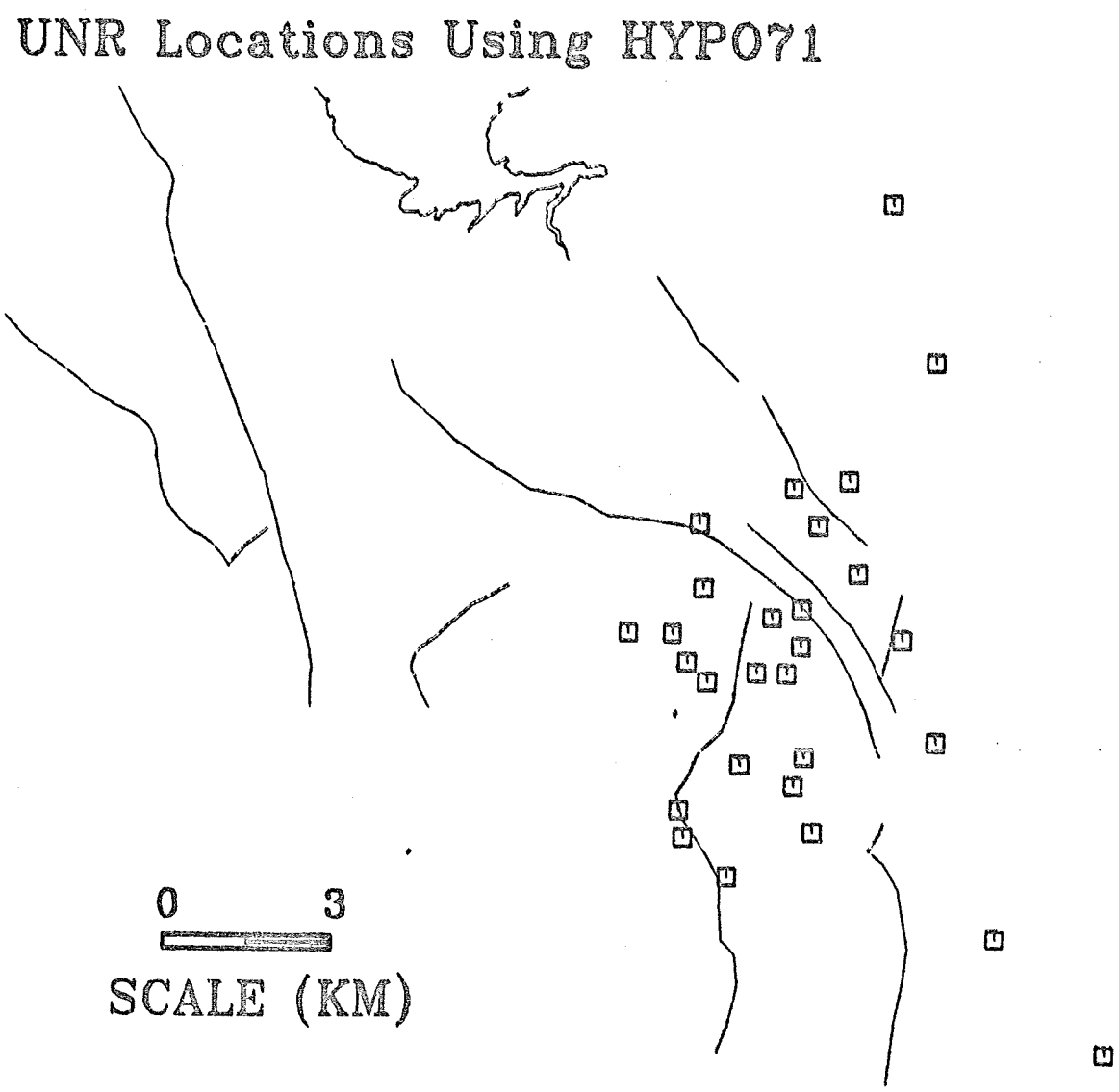

Figure 3. UNR catalog locations of the larger aftershocks of the 04 October 1978 Wheeler Crest earthquake. The stations used for the locations in Figure 2 were a subset of the stations for the locations in this figure (i.e., UNR permanent stations only).

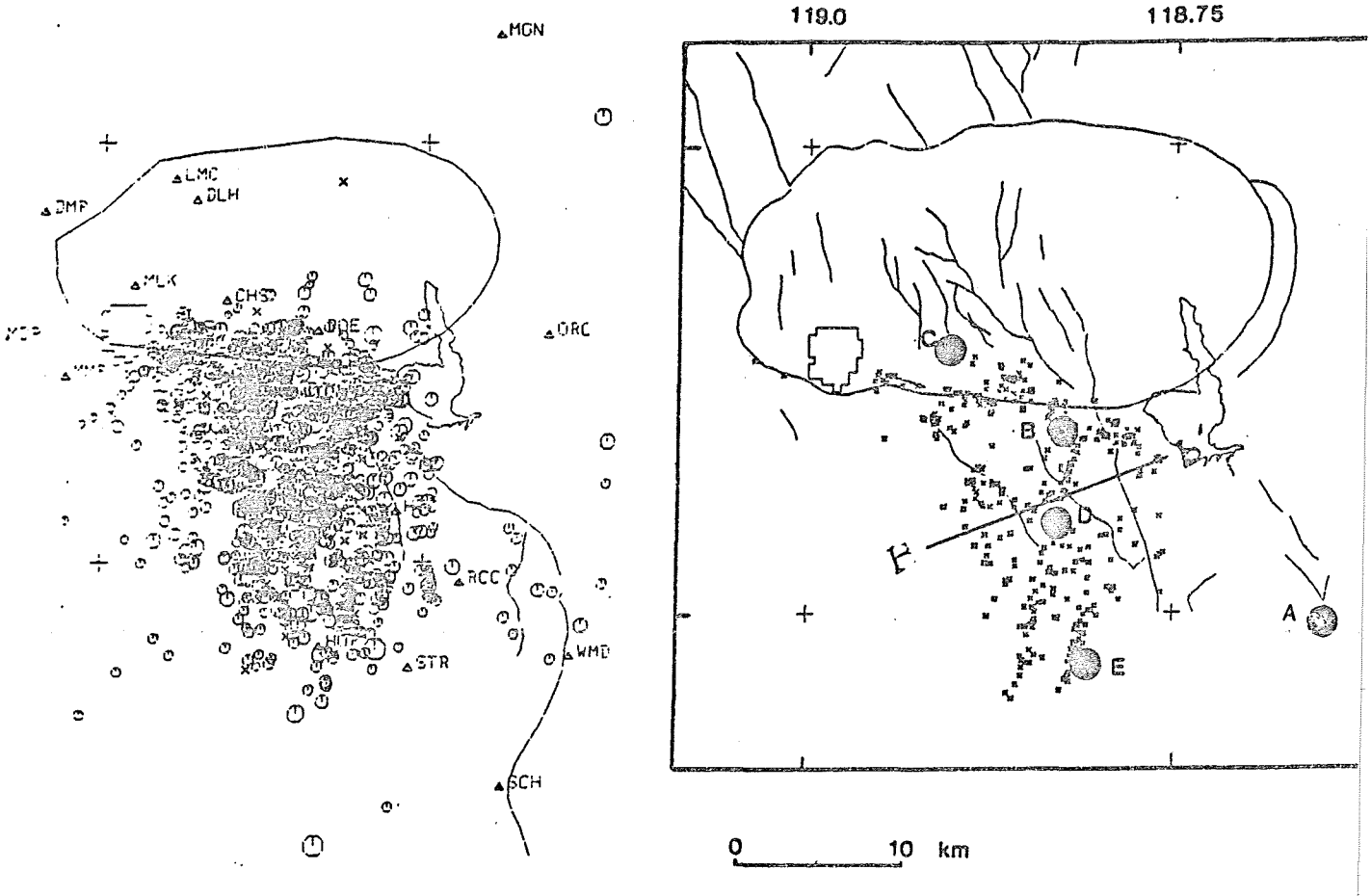

UNR catalog, 1980

Lide and Ryall (1985)

Figure 4. *Right:* Master-event Epicenters of 344 aftershocks of the May 1980 Mammoth Lakes earthquakes whose master-event RMS residual was 0.1 second or less. Solid dots: 25 May 1980, 1633 GCT and 27 May 1980, 1450 GCT (1 and 2, respectively). Master event locations from Lide (1984). *Left:* UNR catalog locations.

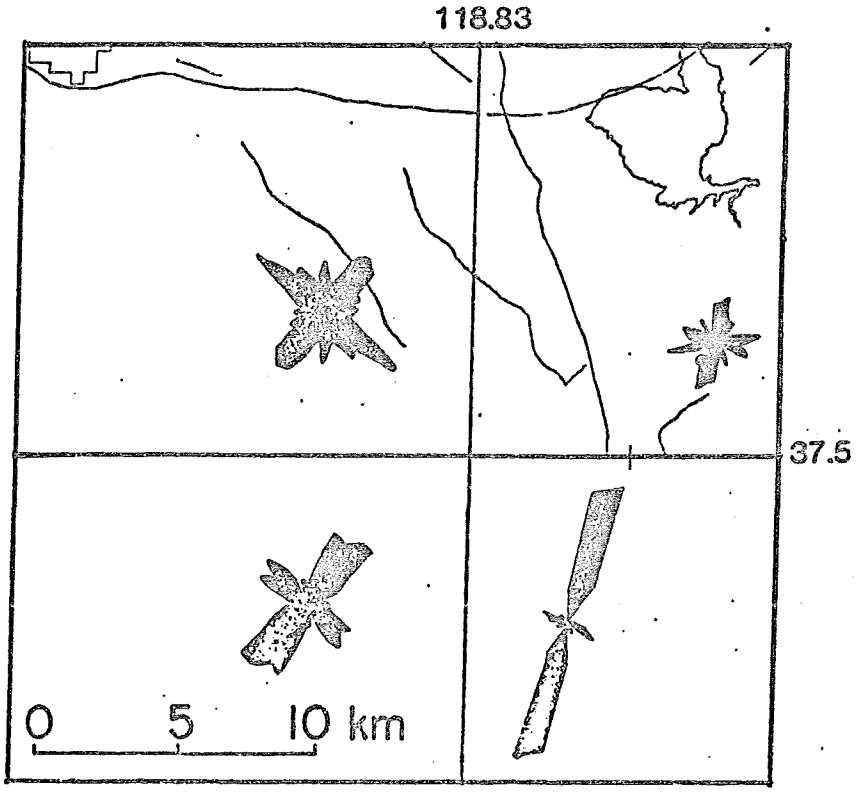

Figure 5. Rose diagrams showing frequency of various orientations of steeply dipping joints and fractures for four areas south of Long Valley caldera, from Mayo (1937).

In connection with our recent contract, these matters are of not inconsiderable interest. For example, a number of authors (Rundle and Whitcomb, 1984) have theorized that the seismicity at Mammoth Lakes is controlled by the injection of magma into the area of the resurgent dome, citing, for example, that the increase in volume as measured geodetically gives about the same order of *volumetric* seismic moment as *shear* seismic moment released by all of the earthquakes. On the other hand, injection of magma may be a passive part of the ongoing tectonics of the region. That is, the forces that now appear to be acting to cause lineups of earthquakes south of the caldera may incidentally be causing the upward movement of magma. Clearly then, this aspect of the contract work has given important new information that will have to be factored into any suggestions on how the seismicity and the magma are related, and we are presently increasing the population of master-event locations for the 1980 sequence to explore these points further.

Another point as noted by C. S. Lide in his thesis is that the seismicity appears to be truncated to the west by a NW trending, W dipping boundary which is on strike with the Hartley Springs fault north of the caldera (**Figure 6**). As this fault is a rangefront fault, this result suggests that there may be a secular migration of seismicity west from what is clearly the eastern boundary of the Sierra front (the Round Valley fault), which will in time lead to a movement of the boundary between the Sierra and Basin and Range tectonic provinces.

1978 Wheeler Crest. Because the 04 October 1978 Wheeler Crest earthquake was the first large event of the sequence, and because Julian (1983) and Julian and Sipkin (1985) have argued for a CLVD non double-couple mechanism for this earthquake, it has recently attracted some interest. Both the University of Nevada and the U.S.G.S. put out temporary stations following this earthquake to record aftershocks. The U.S.G.S. located about 350 aftershocks, mostly deriving readings from smoked paper recordings. We are presently relocating some of these using the UNR data, which can be timed more accurately than the smoked-paper records (timing precision about 0.02 versus 0.05 second for the latter). Somerville and Peppin (1980) have argued that the Wheeler Crest region exhibits characteristics of an asperity, such as found on the San Andreas fault near Parkfield (Bakun and McEvilly, 1979), in that episodes of seismicity which occur along the whole eastern Sierra front from Reno to Bishop appear often to initiate near Wheeler Crest. If this is true, then a better understanding of this source region will be an essential part of unscrambling the tectonics of this region.

2.1.2. On-Line Locations Computed since 1984.

Locations Near and South of Long Valley Caldera

The seismic activity that has occurred since the on-line system started operation in May 1984 is summarized in **Figure 7**. As has been the story since 1980, the majority of the earthquakes have been occurring in the Sierra Nevada mountain block south of the Long Valley caldera. Of the the seismicity that has occurred in the caldera, virtually all of it has been confined to the south moat, and the majority has been located along the south rim fault. This is somewhat surprising because geodetic measurements for the region indicate that deformation is affecting the whole caldera and the center of maximum uplift is towards the center of the caldera.

Within the mountain block to the south, the earthquakes are rather scattered, but a couple of NNE-trending linear features are prominent. These appear to be the result of continuing activity on fault-like features that were discovered among the 1980 aftershock epicenters (Somerville and Peppin, 1980;

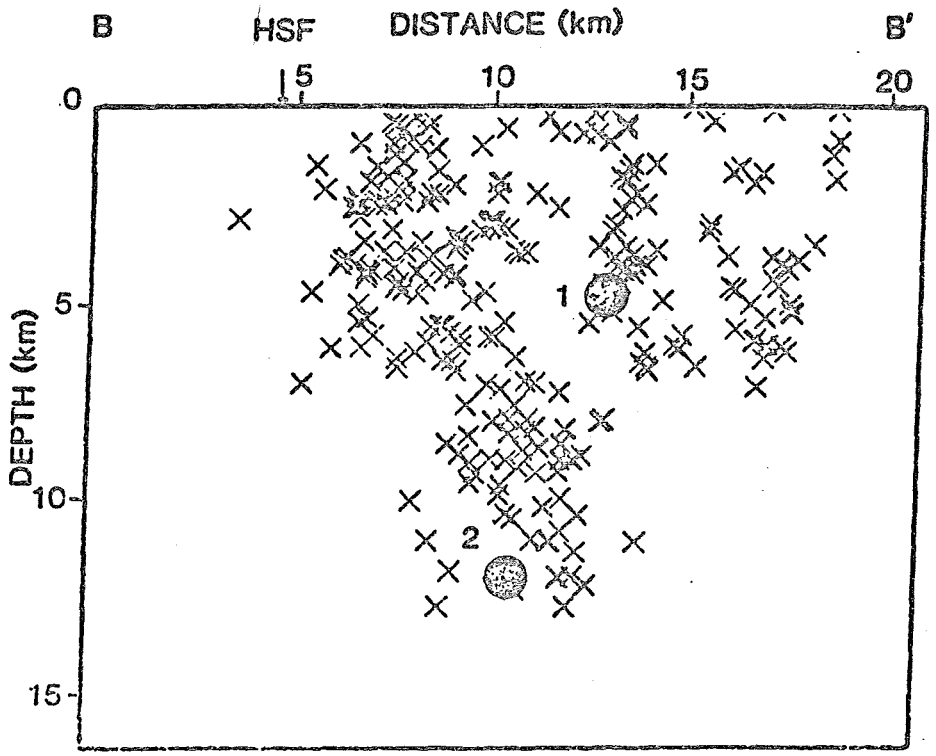

Figure 6. Cross section BB' (see Figure 4) of the earthquakes shown in that figure, with the two large earthquake hypocenters shown as before. "HSF" is the surface projection of the south end of the Hartley Springs fault onto the cross section. From Lide (1984).

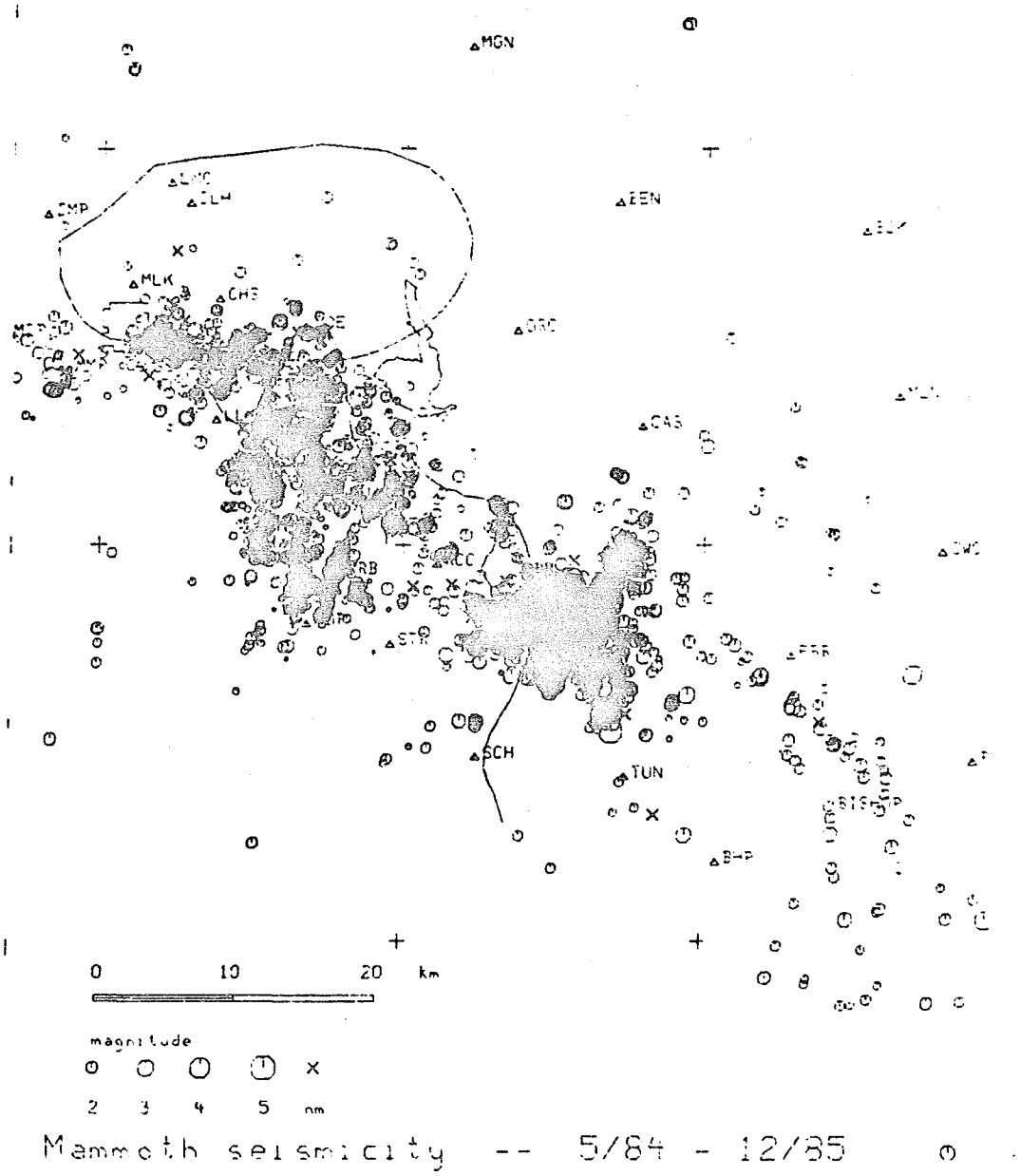

Figure 7. UNR catalog seismicity to date (May 1984 through December 1985) of the Mammoth Lakes region. The same lineations of earthquakes found by Lide (1984), Figure 4 above, are visible, and seismicity at the south boundary of the caldera is greatly reduced relative to a few years ago.

Lide, 1984; Lide and Ryall, 1985). Further to the southeast, earthquakes were numerous in the aftershock zone of the 1984 Round Valley earthquake. The majority of these occurred in late 1984 and the first few months of 1985, and the seismicity was approaching background levels by November, 1985.

Locations of the November 1984 Round Valley aftershocks

As part of our recent DOE contract, our existing seismic network in the Mammoth area was augmented with 10 new stations located south and east of the Long Valley caldera during the summer of 1984 (Figure 1). The intended purpose of these stations was to gather more data on anomalous phases that had been observed for events during the spring and summer of 1984 (see below). These phases had characteristically been observed at stations east of the Sierra Nevada for earthquakes occurring in the Sierran mountain block south of the Long Valley caldera, especially those occurring towards the south end of the Hilton Creek fault. These new stations included five within the Sierra Nevada, whose purpose was to permit accurate locations for the seismic sources, and five stations located 20 to 40 km to the east to hopefully observe the anomalous phases at new sites with similar azimuths. During the late summer and fall of 1984, the seismicity became progressively more quiescent, and no anomalous phases were observed at the White Mountains stations, although some were seen for stations installed in the Pioneer Basin of the Sierra Nevada. Finally, on November 23, a large earthquake occurred right in the center of the new network, the result being high-quality data collected on the mainshock and thousands of aftershocks, yielding excellent control on hypocenters and focal mechanisms. Although the aftershock zone was quite extensive and complex, the many anomalous phases generated by these aftershocks appeared only for events from very localized regions of the aftershock zone. These will be discussed in more detail below, but first this must be put in the context of what has been learned so far about the Round Valley earthquakes themselves.

Round Valley earthquake

At 10:08 am PST on November 23, 1984, an earthquake of magnitude 6.2 M_L (Pasadena) occurred under a broad circular depression known as Round Valley, that is located between the 2-km high escarpment of the Wheeler Crest on the west, and the less elevated depositional surface of the Bishop Tuff (referred to locally as the Sherwin Grade) on the east. The location of this earthquake was not unexpected because it occurred proximate to a major Sierra Nevada range-front fault, the Round Valley fault, which shows well-documented evidence of normal faulting up through the Holocene (Bryant, 1984). However, the evidence gathered from the mainshock and the thousands of aftershocks appears to indicate that the Round Valley earthquake most probably occurred on a fault quite different than the one expressed at the surface.

Initial work presented by Ryall and Hill (1984) and Corbett (1985) showed that the mainshock itself was most probably the result of rupture on a single well-defined fault plane, as indicated by the first 3 hours of aftershock activity (Figure 8). These data suggest that the initial rupture was on a vertical plane trending N 30° E that was 6 kilometers long and extended from 6 to 12 km depth. The location of the mainshock epicenter relative to these aftershocks further suggests that the rupture initiated in the upper northeast corner of this plane and then propogated unilaterally to the southwest and downward. A 3 by 3 km zone of no aftershocks in the vicinity of the mainshock (see Figure 8) has been interpreted as a possible asperity by Corbett *et al.* (1985). Focal mechanisms for aftershocks during the first 3 hours indicate strike-slip motion, with planes trending N 30° E that would correspond to left-lateral movement (Smith *et al.*, 1985). A first-motion fault plane solution was not obtainable for the

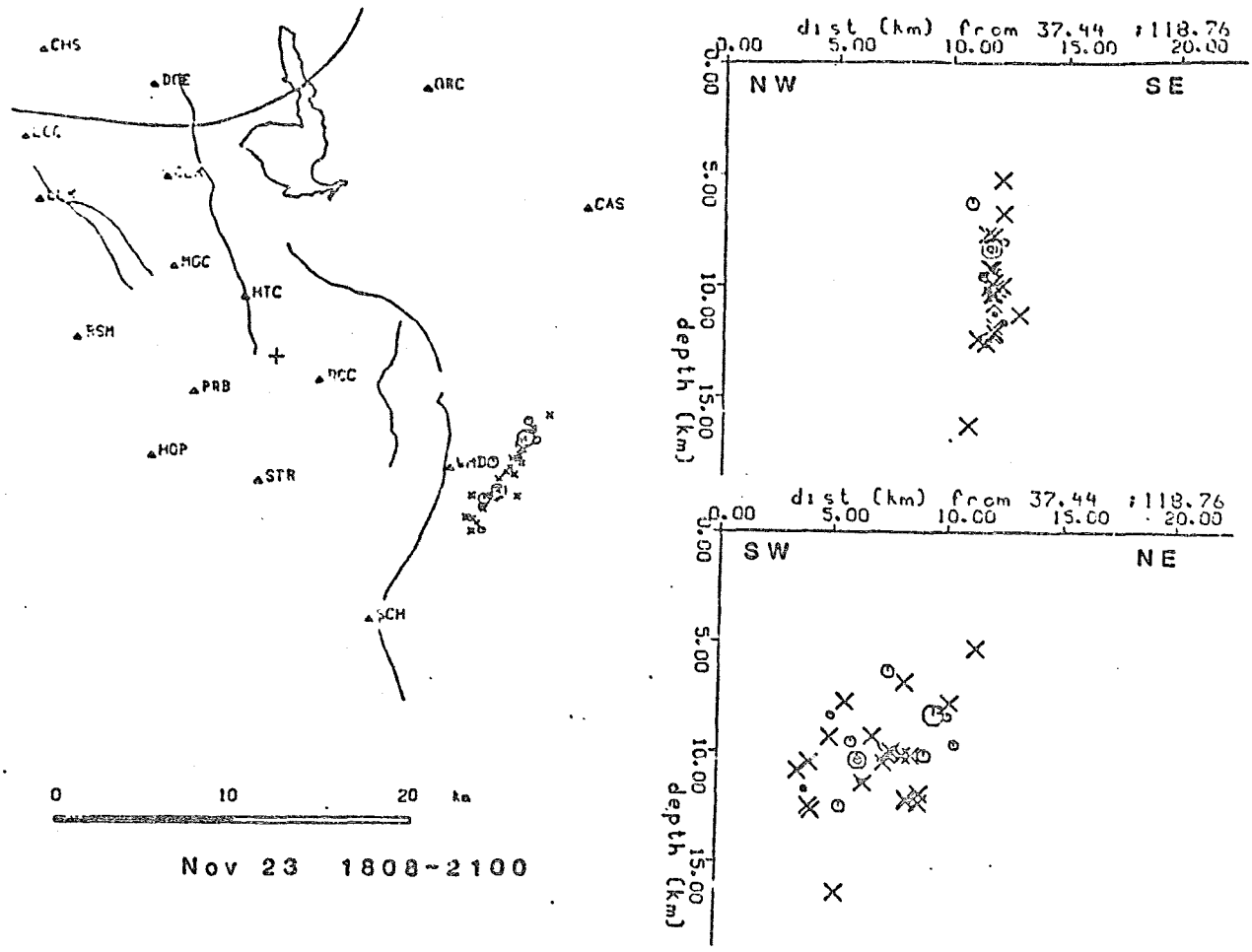

Figure 8. Seismicity and cross sections across (NW-SE) and along (SW-NE) a NE lineup for the first three hours following the 23 November 1984 Round Valley earthquake.

mainshock due to a foreshock preceding it by 4.5 seconds. However, Barker and Wallace (1985) have performed an inversion on the teleseismic body waves for this event which also indicates left-lateral faulting on a NE-trending plane.

After these first few hours of activity, aftershocks began to occur frequently off this main trend and at shallower depths, so that this simple zone quickly grew more complex. After three weeks the aftershock zone was a 12-km sided triangle with the initial NE trend still apparent as the main structure (**Figure 9**). Cross-sections of these data show that most of the off-trend activity is shallower than 6 km and tends to get progressively shallower to the NW (**Figure 10**). There is also a somewhat weaker suggestion of a planar structure that dips 80° to the NE and trends NW from the south end of the original fault rupture. Fault mechanisms for these shallower events show that these are predominately vertical-slip or oblique-normal events. Both of these types of mechanisms contain NE-trending planes, but they would correspond to down-to-the-west movement, which is at odds with the Quaternary tectonics that is observed at the surface. Due to the NW-trending line-up of some of the shallow normal events, one has the option of choosing down-to-the-northeast movement on NW-trending planes, but this trend is nearly perpendicular to the range-front fault at this point. In short, the many aftershocks that occurred off of the principal strike-slip trend suggest a complicated process of tectonic stress release that is quite different from the initial mainshock rupture as well the Holocene surface faulting. A possible explanation is suggested by Corbett *et al.* (1985), who note that the aftershock seismicity propagates westward and upward as a function of time. They suggest that this phenomenon is the result of pervasive fracturing of the shallow crust in response to the temporal migration of stresses and/or fluids. Although the presence of magmatic fluids is well documented under the Long Valley caldera, it is surprising that they may be located this far to the south, especially in light of the lack of extrusive rocks younger than the Bishop Tuff (0.7 m.y. age) and the absence of geothermal activity in this area. Thus, we have made an effort to determine the relationship (if any) with magmatic activity south of caldera.

2.2. Focal Mechanisms.

The November 1984 Round Valley earthquake offered an excellent opportunity to study a large number of first-motion earthquake focal mechanisms using a dense array with good azimuthal coverage. Results have appeared in a number of abstracts (see below). Several points are of interest. *First*, as with the other earthquakes of the Mammoth Lakes sequence, the mechanisms show no correlation with prominent geologic features of the area, *second*, the pattern of focal mechanisms is distressingly (not to be facetious) complex, and *third* they have provided information about the extent of the unique Mammoth Lakes stress regime. These are discussed in sequence.

Poor Correlation with Surface Features. As for the 1978 and 1980 aftershocks, we again find that a definite vertical fault plane appears to be shown by the early aftershocks, and the focal mechanisms on this plane are consistent with its strike (see Figures 2 and 6 above). But as with the 1980 earthquake aftershocks of Lide (1984), this plane shows absolutely no correlation with any mapped fault. Because the earthquake occurs to the east of one of the major range fronts of the western U.S., with some 2,500 meters of very steep relief, we might have expected to see expression of normal faulting in connection with this earthquake, consistent with the sense of substantial, obvious Holocene normal faulting that can be seen all along the eastern Sierra front (and which was manifested only a few tens of km south in the great earthquake of 1872). To make

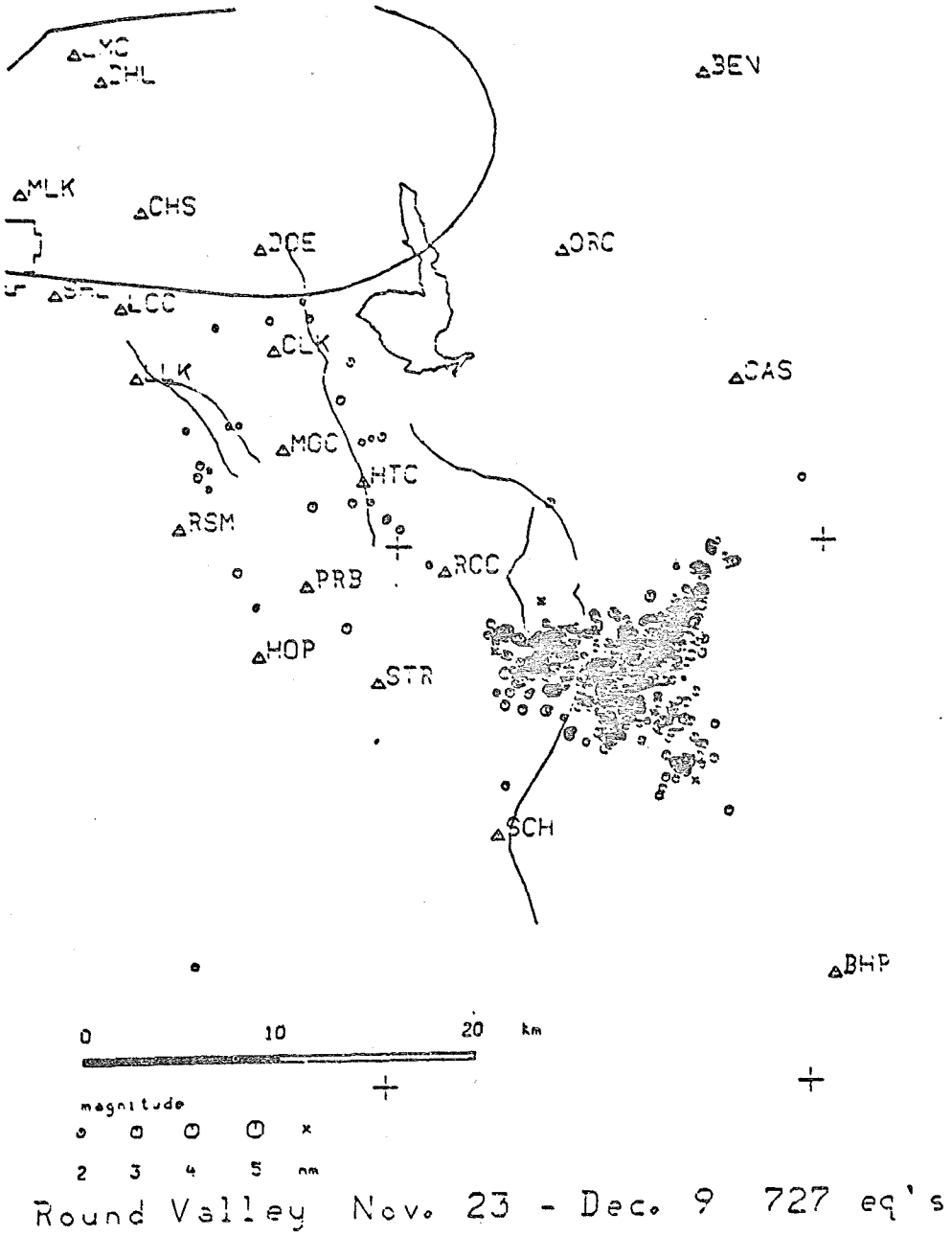

Figure 9. Seismicity comprising most of the aftershocks of the 23 November 1984 Round Valley earthquake showing the expansion of the aftershock zone.

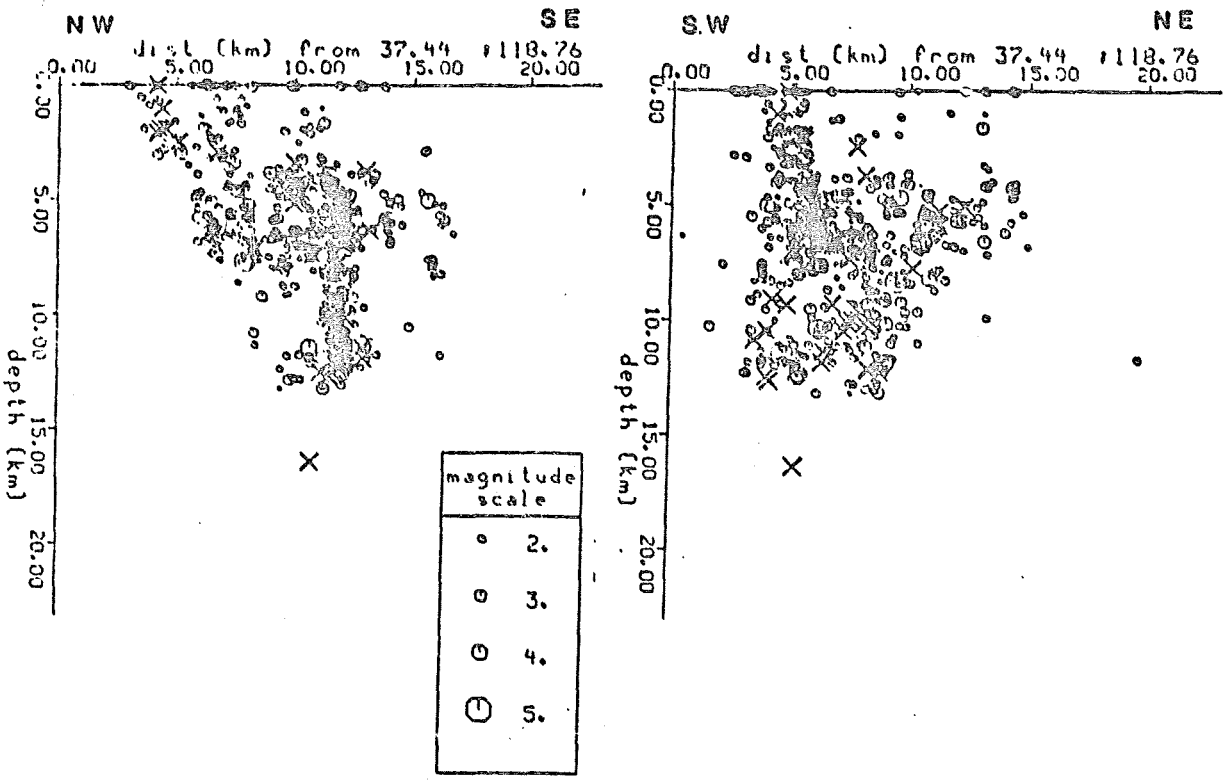

Figure 10. Cross sections for the seismicity shown in Figure 9. The figure shows that the NE trend is mainly earthquakes 5 to 12 km deep, and the earthquakes occurring off this trend have shallower hypocenters in general.

matters worse, the aftershock sequence does indeed show quite a few normal-faulting mechanisms: but for these the west side (toward the mountains) is down. In no other area of the Basin and Range where magnitude 6+ earthquakes have occurred (Yellowstone; Borah Peak; Hansel Valley; Dixie Valley; Fairview Peak; Pleasant Valley; Cedar Mountain; Owens Valley) is there such complete lack of correlation of the aftershocks with mapped normal faulting features. It is possible to argue that this is in itself evidence for seismicity strongly influenced by other than the normal extensional tectonics of the Basin and Range (i.e., by recent intrusion of magma).

Focal Mechanism Complexity. The work of Corbett (1985) Smith *et al.* (1985) shows that the pattern of focal mechanism associated with the Round Valley earthquake is very complex. After a quite simple start, in which most of the earthquakes were NE trending strike-slip mechanism (consistent with the NE trend of the early aftershocks), the aftershock pattern grew quite complex, and produced a wide variety of mechanisms. It appears that at least a part of this complexity arises from the fact that the mainshock appears to be located in an asperity of several kilometers extent. In one respect the Round Valley earthquake is "ordinary": focal mechanisms obtained from the teleseismic inversion of P-waves (Barker and Wallace, 1985) give a focal mechanism consistent with strike slip motion on a NE trending plane. This complex pattern of focal mechanisms shows that we must definitely be careful when extrapolating results obtained from small earthquake aftershocks to make statements about the regional stress field. This complexity may be the result of very localized block movements caused by highly fractured rock, and therefore not representative of regional tectonics, but rather a manifestation of what amounts to complexity in near-source rheology. In fact, we can be hopeful that detailed examination of microearthquake focal mechanisms in this area might be used for just the purpose of studying this rheology.

Stress Regime Boundary. One of the interesting points about focal mechanisms of the Mammoth Lakes earthquakes is that, uniquely among Basin and Range earthquakes, they show dominantly NE-trending axes of extension, where Basin and Range tectonics is consistent with extension in a WNW to westerly direction. That is, in a rather small area 50 by 30 km in extent, and centered on the Long Valley caldera, the directions of extension obtained from focal mechanisms is different from surrounding regions (EW, or San Andreas style extension to the west and WNW-ESE, or Great Basin style extension to the east). Pitt and Steeples (1975) presented composite microearthquake focal mechanisms for the northern end of Owens Valley and reported a rotation of the tension axes for Mammoth, as compared with Round Valley events.

With the occurrence of the 1984 Round Valley earthquake, we were offered the chance to reexamine this situation much more critically. Recent work by Vetter (1986) is summarized in Figure 11. Shown are stereo plots of the axes of compression and extension for two groups of well-controlled focal mechanisms (top) and frequency-versus-azimuth plots of the strike of the focal planes (bottom). The events on the left are west of the Round Valley fault, under Pioneer Basin; the events on the right are east of the Round Valley fault in the aftershock zone of the 1984 event (Figure 9). The Pioneer Basin events are typical of others with the characteristic ENE extension axes of caldera events, while the Round Valley events are more variable. It is notorious that almost no mechanisms occurring west of the Round Valley fault show the WNW axes of extension that typify earthquakes of the Basin and Range (and reflected in the regional geology with NNE trending basins and ranges). Therefore, it can be suggested that the Round Valley fault forms the precise boundary between the Mammoth Lakes tectonic province and the Basin and Range, and that the transition to

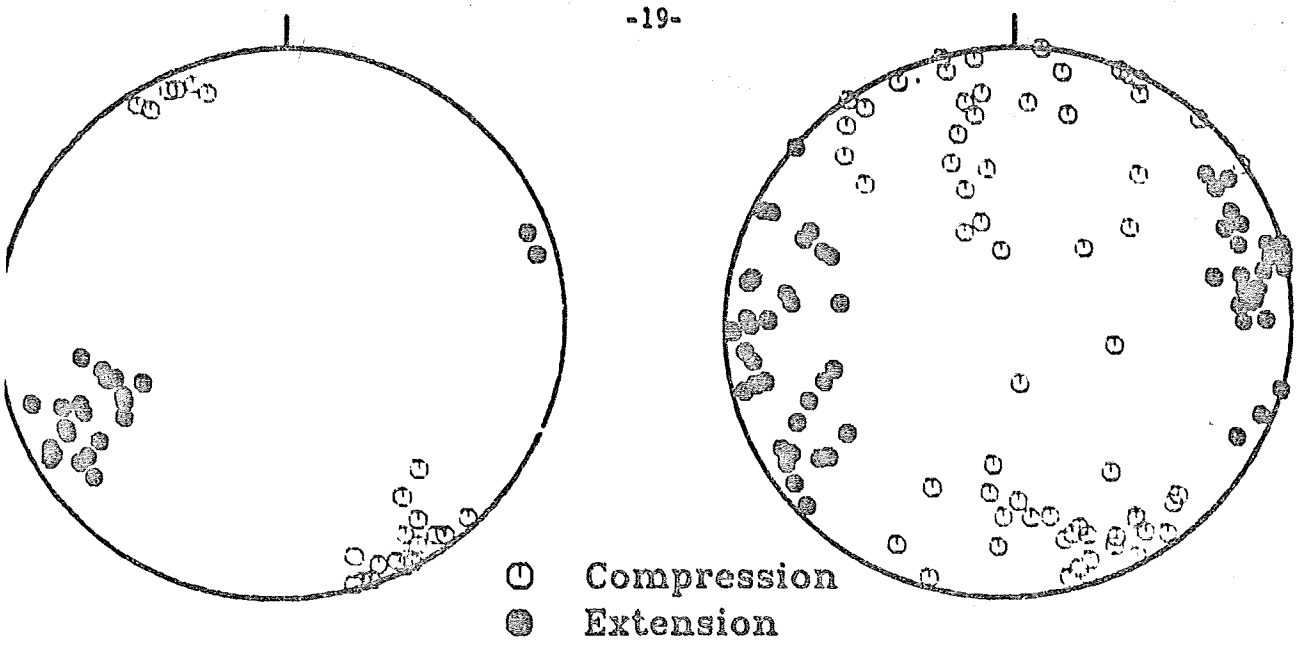

PRB Stress Axes

WMD Stress Axes

PRB Focal Planes

WMD Focal Planes

Figure 11. Characterization of focal mechanisms of the Round Valley aftershocks. The events on the left are those which occur in the mountain block in the vicinity of station PRB, while those on the right occur in the aftershock zone of the Round Valley earthquake as shown in Figure 9. The diagrams above are stereo plots of the axes of compression and extension; the diagrams below are rose diagrams of the frequency of occurrence of focal planes with the indicated strike. From Vetter (1986).

Basin and Range occurs in a more diffuse zone extending east perhaps to the White Mountains. If true, this hypothesis would provide a substantive constraint on tectonic models proposed for this area.

2.3. Waveform Analysis.

During the recent contract period a considerable amount of work was done on waveform analysis. "Waveform analysis" in this context means the analysis of seismic travel times and the general character of waves rather than the meaning currently understood by seismologists, i.e., comparison of theoretical with observed seismograms. Although we are now on the verge of doing some such comparisons based on our accumulating data base and knowledge of these waveforms, no such work was attempted in the recently-ended contract period. Much of the material in this section was presented by Peppin (1985).

2.3.1. S-Wave Shadowing. As noted above, a primary motivation for the funding of research at UNR by DOE was the work on S-wave shadowing. The result of this work has been the only definite proposal yet published (Sanders, 1984) delineating shallow-crustal anomalies in Long Valley caldera which most investigators now accept as magma bodies. At a recent contractors' meeting involving the proposed deep hole drilling project within Long Valley, discussion centered around Sanders' work, because it provides one of only two lines of evidence that would now permit placing a mark on a map and sinking a hole to reach magma (the other line of evidence being the location of the January 1983 earthquake swarm near Casa Diablo). Recent work by Ryall and Ryall (1984) presented evidence for a number of crustal anomalies south of the caldera under the mountain block (Figure 12). Because of the recent deployment of many recording stations in this region, our efforts have concentrated here, although we have maintained our watch for S-wave shadowing related to the caldera itself. However, we note that we have seen relatively few examples of S-wave shadowing since initiation of the on-line system (a few dozen examples in 50000 traces). Most of the past work on S-wave shadowing was done by F. Ryall, who discontinued her efforts fairly early in 1985; this probably explains in part why our catalog has few such observations. Because of interest in this phenomenon, we are now developing a method to do a computer search, based on spectral ratios and statistical criteria, so that the analysis method can be made more objective and repeatable. Our efforts have deemphasized S-wave shadowing because we have been focussing on what appear to be more promising methods (see below). A significant problem with the method is that we almost never see S-wave shadowing for short travel paths. In fact, the DOE-supported stations placed along the western boundary of the White Mountains were located with the idea of obtaining shadowed records to those azimuths, but so far not a single example of shadowing at those stations had been observed. Therefore, the problem is that, even if shadowing is seen, the travel path is so long that it is quite difficult to pinpoint the location of the causative crustal anomalous zone. In fact, this is the main reason why various investigators doubt the *accuracy* of the map locations of the Sanders (1984) proposed magma bodies.

2.3.2. Post-S Phases.

During the present contracting period we have recorded some 40 examples of an extraordinary phase that comes in very strongly and quite a bit behind the S wave at only one station (Benton). Hereinafter this phase is called the *Benton phase*. The epicenters of earthquakes for which this phase were seen are shown in Figure 13. We see that these events cluster mostly in a region west of the Hilton Creek fault (HCF) and south of the caldera.

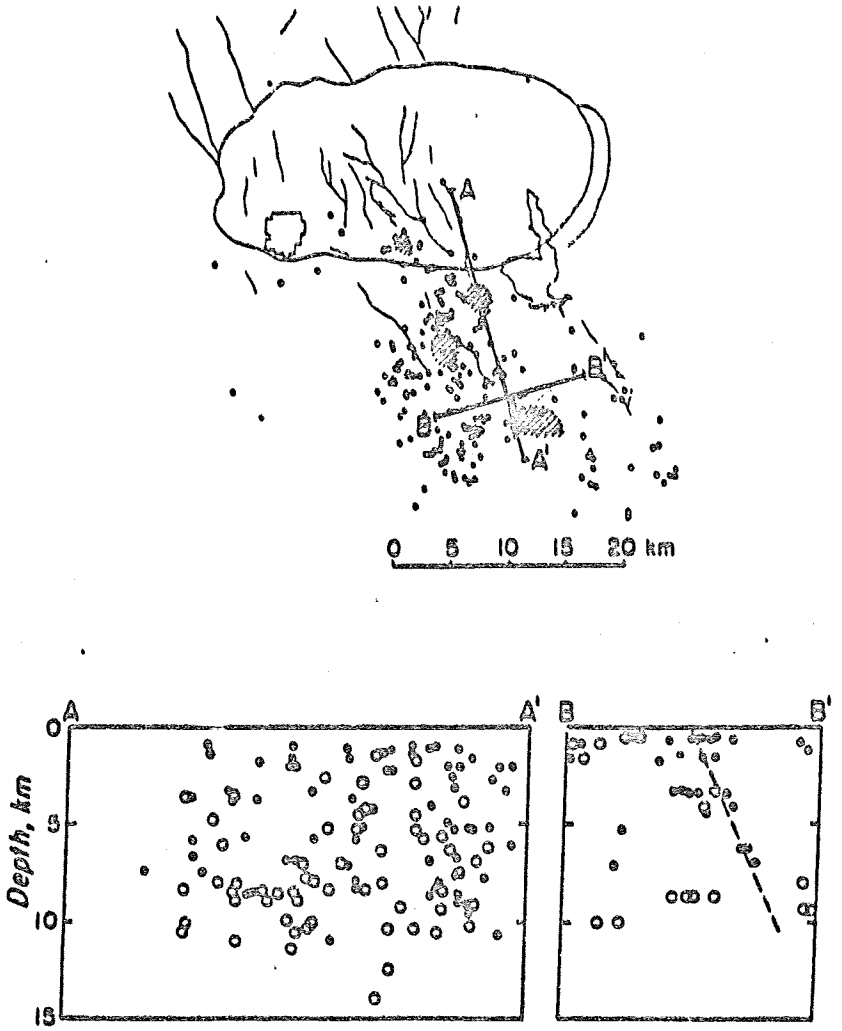

Figure 12. Summary of earthquakes used to delineate attenuating bodies south of Long Valley caldera. The events used in the analysis are shown as solid dots (top image). In the bottom image, showing sections parallel and perpendicular to Hilton Creek Fault (HCF), the solid dots are the projections of earthquakes which show S-wave shadowing and the open circles show earthquakes producing normal seismograms. There appears to be an association of the events causing shadowing with the inferred projection to depth of HCF, given as the dashed line in the lower right section BB'. From Ryall and Ryall (1984).

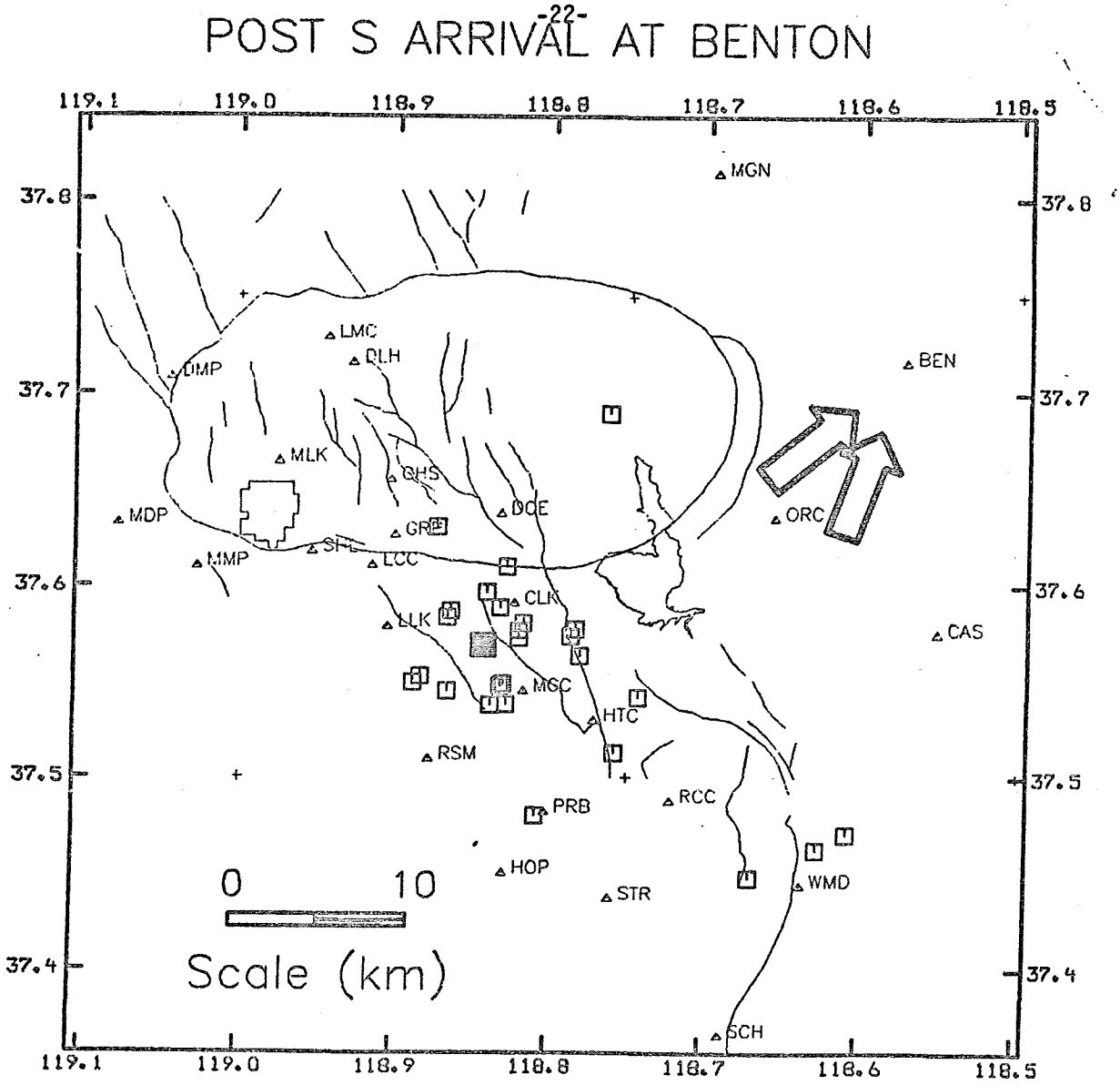

Figure 13. Map location of those earthquakes producing the strong post-S phase at station Benton (BEN in the figure as indicated by the large arrows). Solid dot: earthquake of 15 August 1984 at 1650 GCT. The top arrow is the direction from the source to the receiver, and the bottom arrow indicates the approximate direction motion as indicated by Rayleigh-wave particle motion of the Benton phase.

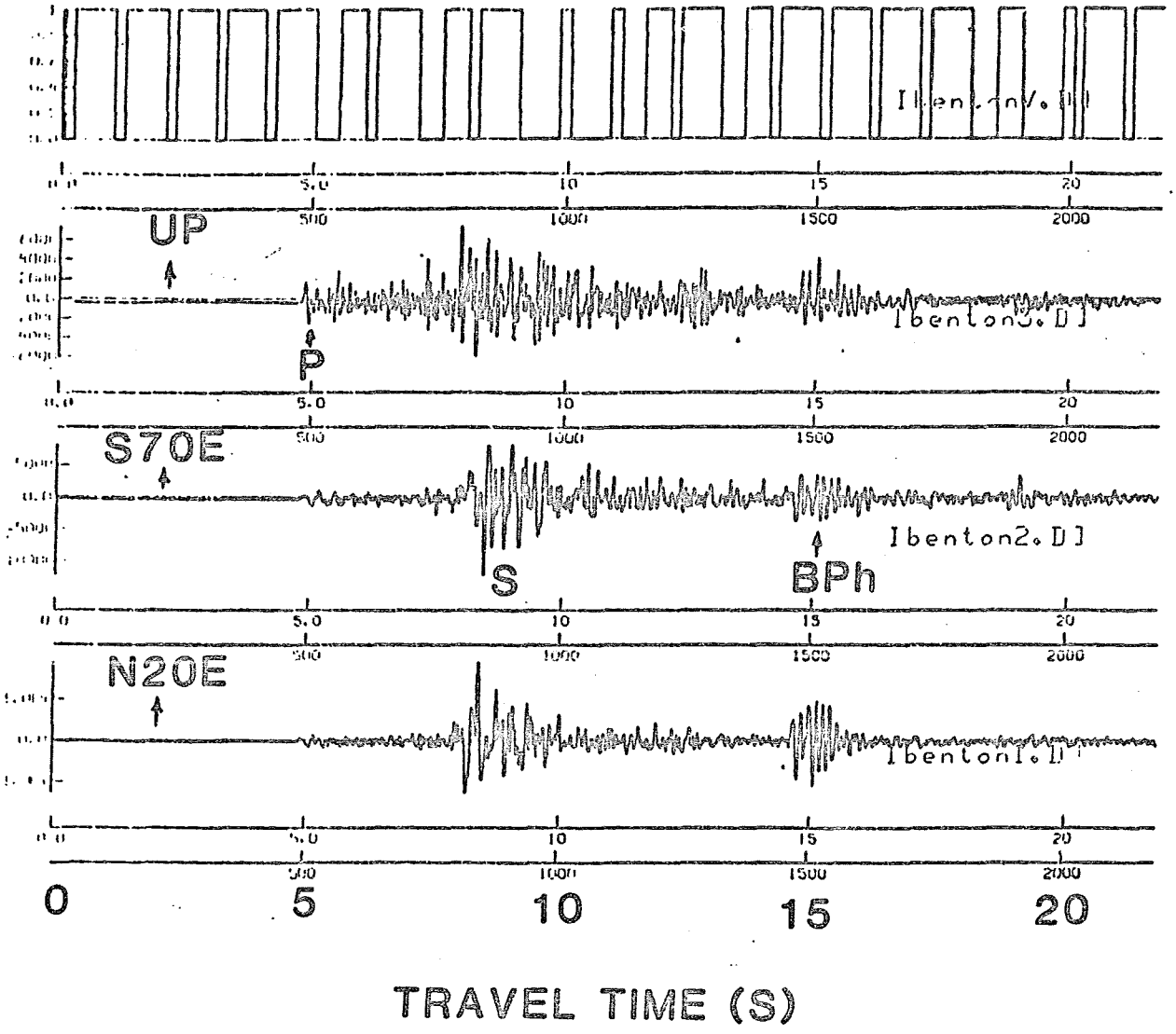

Figure 14. Whole-record seismograms taken on a digital wideband event recorder for the earthquake of 15 August 1984 at 1650 GCT. The P and S arrivals are labelled P and S, while the Benton phase is labelled BPh. The direction of particle motion is indicated on the traces.

In order to understand the nature of the Benton phase better, a 3-component wideband digital seismograph was placed, alongside the existing telemetered short-period vertical instrument on which the phase had first been noted. Traces as recorded for the earthquake of 15 August 1984 at 1650 GCT are shown in **Figure 14.** The Benton phase is the large arrival, seen about seven seconds later than S. The location of this earthquake is indicated also in Figure 13.

Consider first the particle motions of the P-wave as compared with the later Benton phase. In **Figures 15 and 16** we present blown up versions of the three components for closer analysis. We see (Figure 15) that the P-wave moves up, N and E, i.e., longitudinal in the direction from the source to the receiver, which is from the SW. On the other hand, the Benton phase (Figure 16) shows particle motion on the horizontal components which is dominantly in the direction about N 20° E, some 30 degrees counterclockwise from the direction of P. Moreover, note that the vertical component (top trace) is shifted 90 degrees in phase from the two horizontal components. Therefore, this motion has the characteristics of a Rayleigh wave whose direction of advance is from S 20° W. As corroboration, notice that the bottom two components in Figures 14 and 16 show a fairly obviously dispersed wave train, typical of surface waves. However, this cannot simply be a Rayleigh wave that travelled directly from the source to the receiver, because the arrival time is much too late (note that the interval *Benton - S* is double the interval *S - P*). We are forced to conclude that the travel path is complex.

We had originally thought that the Benton phase originates as a lateral reflection off a strong vertical discontinuity in Long Valley caldera (e.g., from one of Sander's, 1984 magma bodies). However, the sense of Rayleigh wave motion has the direction of advance from S 20° W, which is the general direction of the south end of HCF. It is notorious that the Benton phase is seen on almost no other station, including stations closer or beyond Benton on this same azimuth such as ORC (see Figure 13). It appears to us that the strong selectivity of the Benton phase (revealing itself only at that station) results because of a strongly azimuthally-dependent focussing effect by waves incident on a curved (cylindrical?) velocity anomaly near the south end of HCF. The kind of scattering model we have in mind is suggested by the ray tracing models shown in **Figures 17 and 18.** In these figures we show the effect of scattering of rays from either a perfectly planar interface or a geometry about of the scale and type we are thinking of, namely a cylinder a few km in extent with some undulations (to simulate first-order deviations from a perfect cylinder). The second diagram shows how the rays can focus and defocus at many different distances and azimuths, and, in particular, how, by coincidence, amplification could appear at an isolated station like Benton.

2.3.3. Pre-S Phases South of the Caldera. During the past contract period we have found 70 examples of yet another pattern in waveforms that has puzzled us for seven years: the existence of strong phases occurring between the P and S-waves of earthquakes south of Long Valley caldera. A summary of these observations is given in **Figure 19.** In **Figure 20** is shown an example which is a paradigm of this phenomenon. At all stations where it is recorded, the phase has the same general appearance as the P-wave (S usually having visibly lower frequency content). Where three-component records are available, the phase appears strongest on the vertical component. Considering the records shown, we note that the phase must almost certainly be caused by a lateral reflection (low incidence angle) because it is so strong (for certain events this phase is the largest on any of the three components), and because the sources are almost directly under the recorder. Note that a reflection from below the source is

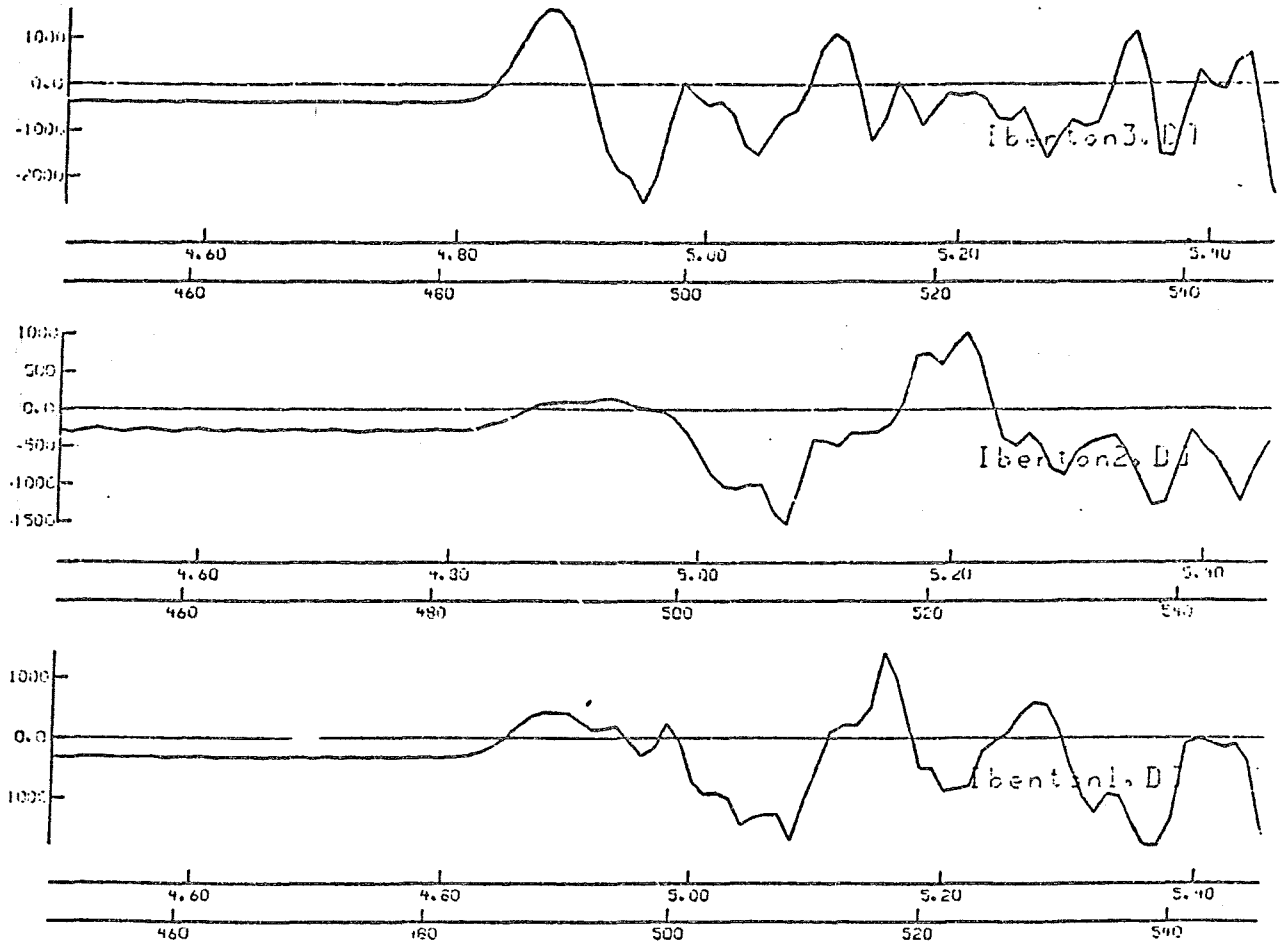

Figure 15. Blow-up of the P-wave portion of Figure 14 showing direction of advance from roughly the southwest.

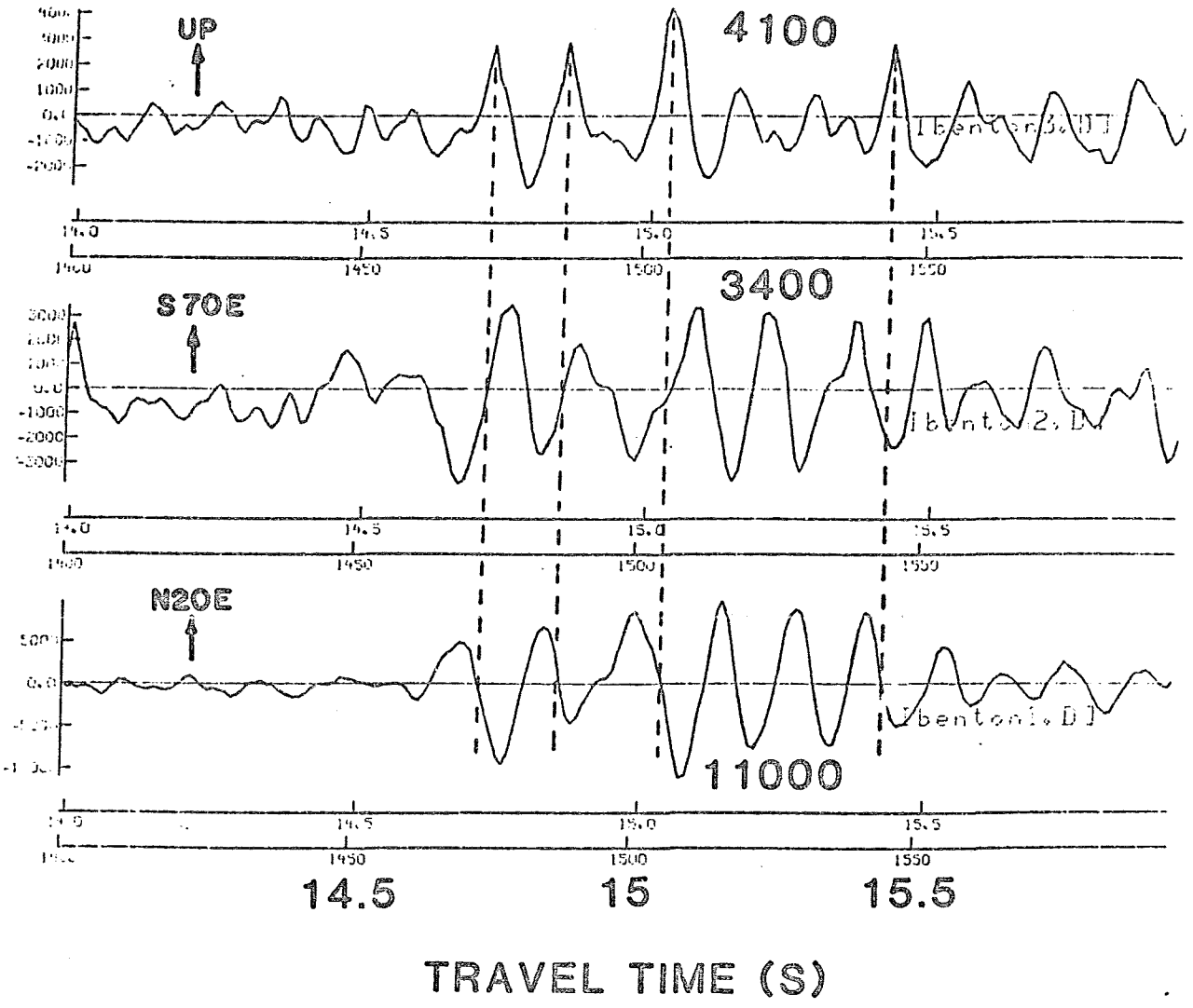

Figure 16. Blow-up of the Benton phase portion of Figure 14. Numbers above each trace are the maximum trace amplitudes (the N20E component dominates). We see that the direction of approach of the Rayleigh waves is dominantly from S20W.

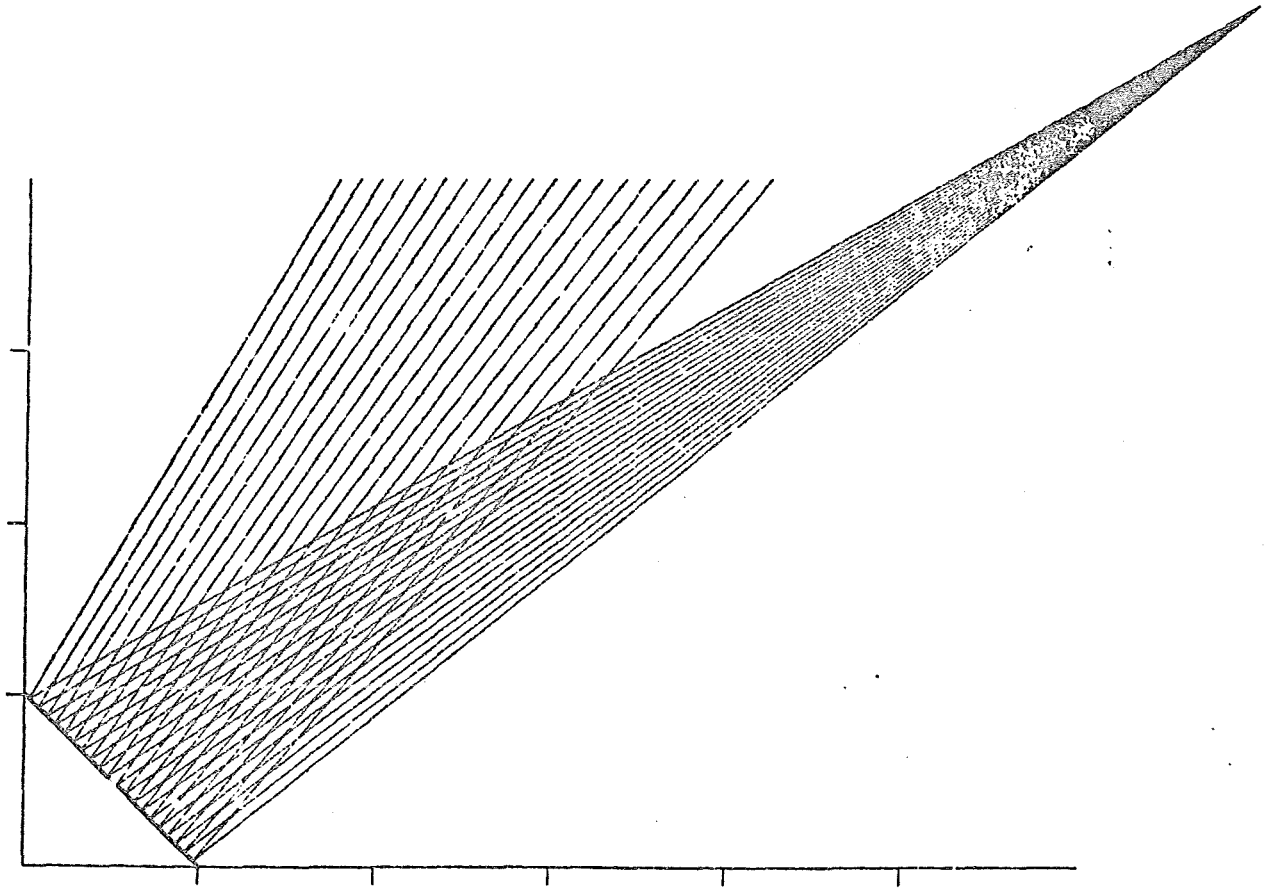

Figure 17. Ray tracing showing reflection from a flat-lying reflector. Because of the assumed smoothness of the reflector, the reflected rays are uniformly spaced.

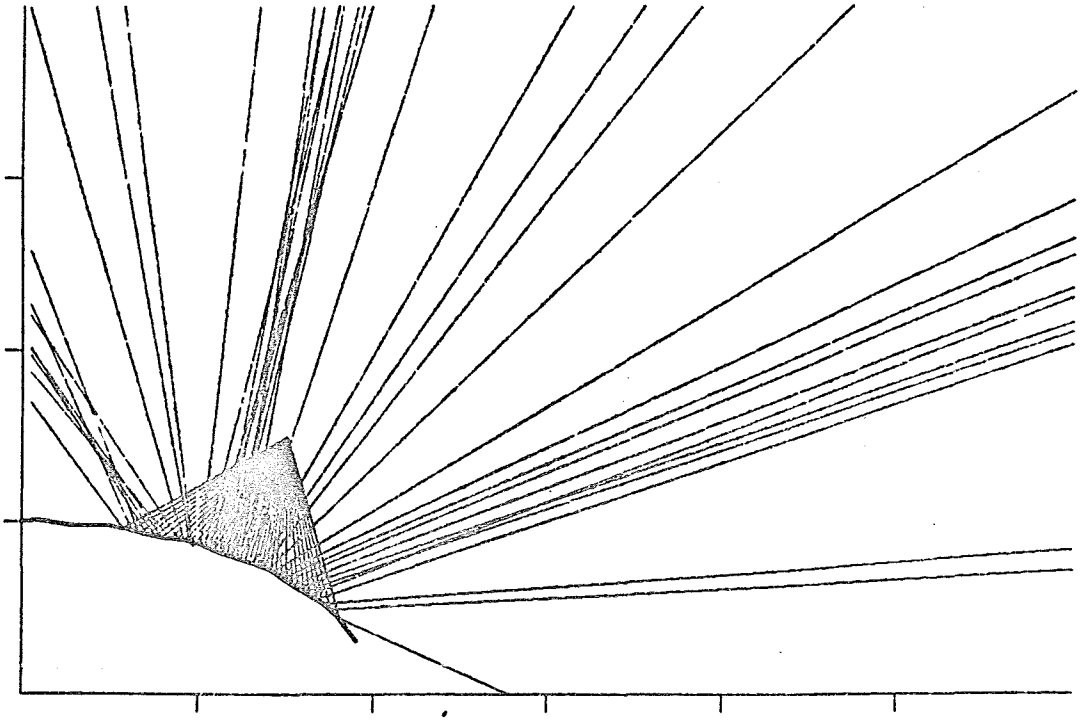

Figure 18. Ray tracing showing reflection from an elliptical boundary with some irregularities. There is striking focussing and defocussing of the ray energy with both distance and azimuth. We suppose that Benton lies at a point where there is focussing of reflected energy relative to the south end of Hilton Creek fault (however NOTE that this is far from a unique explanation for this phase).

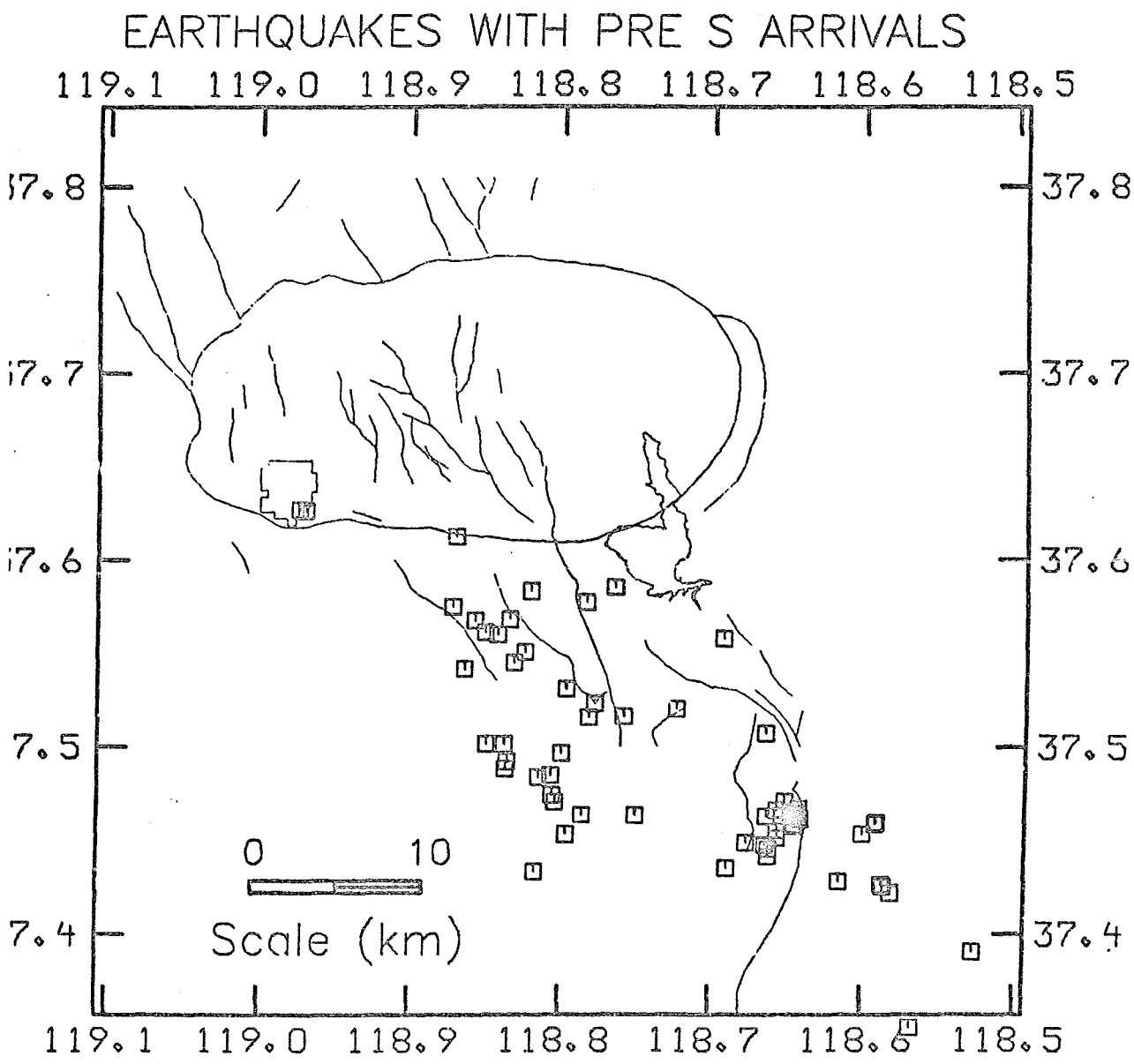

Figure 19. Map locations of earthquakes south of the caldera showing pre-S phases on stations south of the caldera.

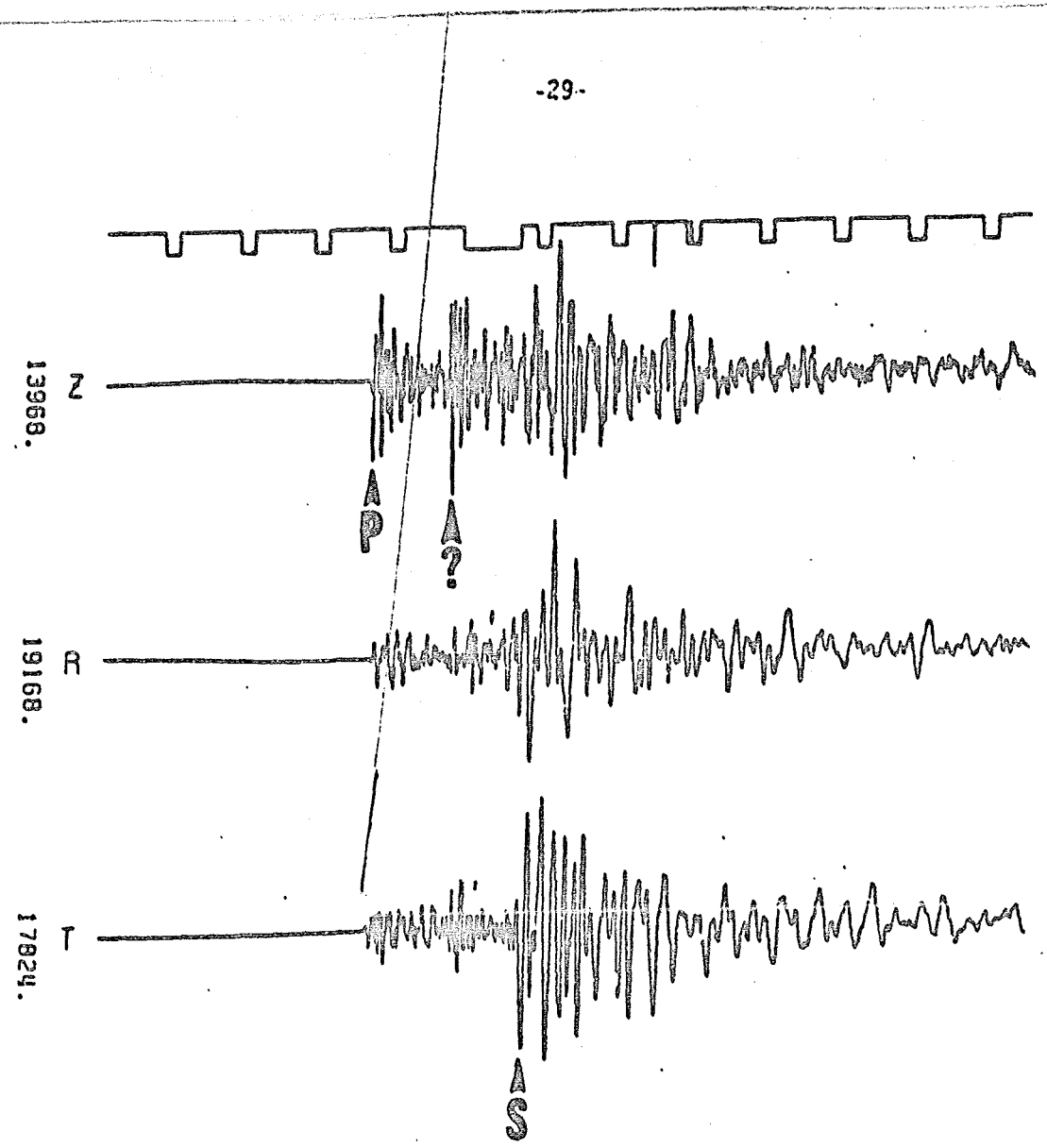

Figure 20. Digital event recorder seismograms of an aftershock of the 04 October 1978 Wheeler Crest earthquake, station BIW. Top trace: WWVB time code; bottom three traces: vertical and two horizontal components of ground velocity in the band range 0.1 to 50 Hz. Numbers left of each trace denote maximum trace amplitude (digital counts). The P and S arrivals have been identified, along with the pre-S phase labelled "?" on the vertical component. The earthquake is 13 km deep almost directly under the recording site. About 30 records like this were obtained for a distribution of aftershocks several km N and S of the recording site.

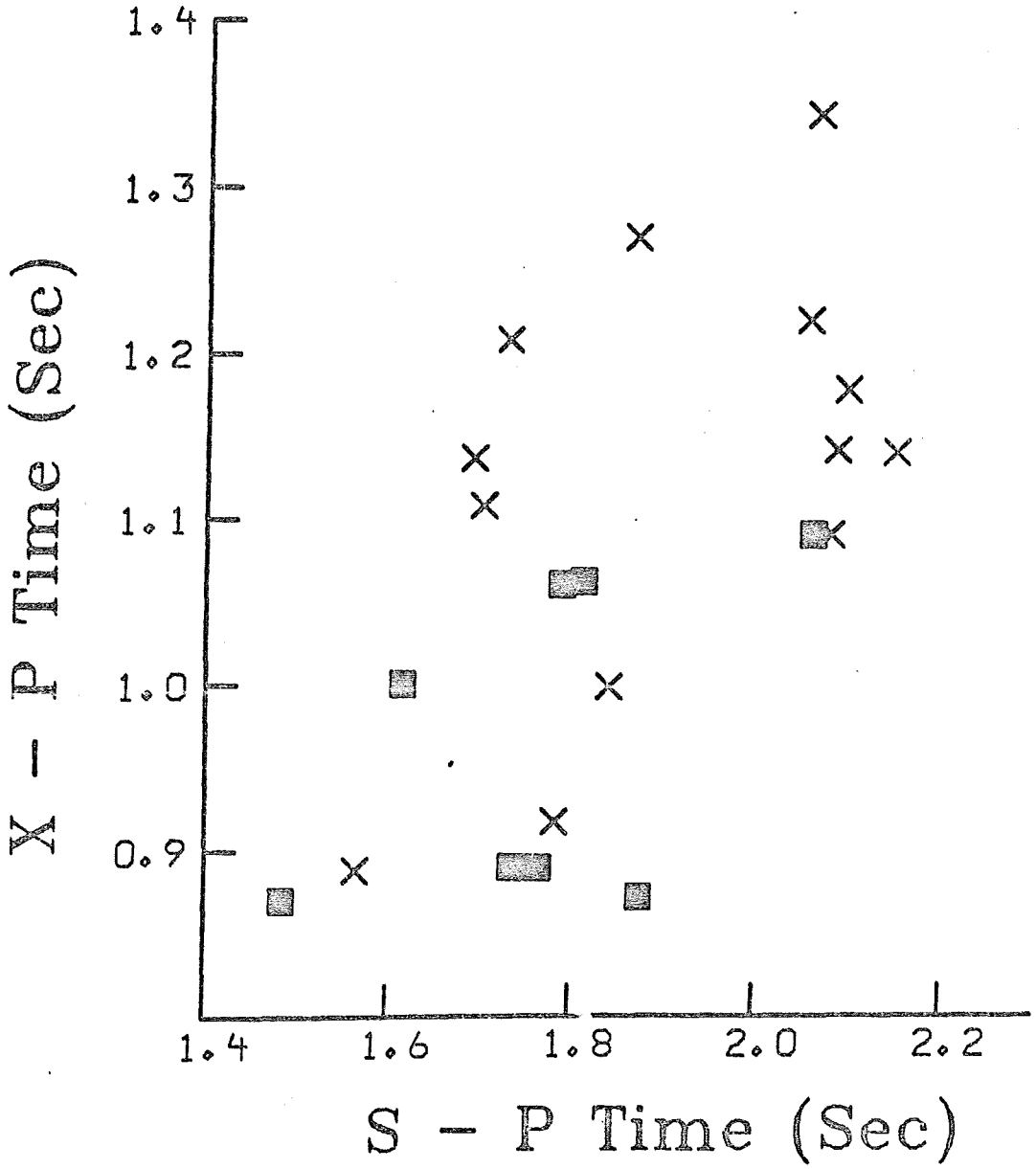

Figure 21. Plot of S-P versus X-P time in seconds, where "X" is the pre-S arrival shown in Figure 20. Note that the X-P time appears to increase with S-P time, which eliminates a number of possible explanations for this phase (such as a reflection from a flat-lying layer below the sources of the earthquakes).

ruled out because the moveout time of the phase relative to the P onset weakly increases with the focal depths of the events, as we can see from Figure 21: a reflection from below the sources would show a decrease in X-P interval for an increase of S-P interval. Comparing Figure 19 with Figure 9 we see that only a small fraction of the aftershocks of the Round Valley earthquake produce pre-S phases within the UNR network, and that the Round Valley fault, just west of station WMD, serves as a rather sharp boundary between the earthquakes that show the phase (to the west) and those that do not (to the east of the fault).

Of all the unusual phases seen on seismograms taken in and near Long Valley caldera, these pre-S ones are unique in that they are seen over comparatively short travel paths (often at epicentral distances comparable or smaller than the hypocentral depth). This provides the potential to locate the source of any causative crustal anomaly quite precisely. We are now performing master-event relocations of those earthquakes which showed a pre-S reflection at the 3-component digital station BIW (Figure 20). One interesting observation (Figure 22) is that the earthquakes which show the pre-S phase most strongly at BIW cluster in two widely separated groups.

Figure 23 is a map showing the occurrence of pre-S phases by station. It is remarkable that the stations showing the observation most frequently are grouped around the south end of HCF, with station BIW the one at which the phase has been seen most often.

As another indication that the south end of HCF is intimately associated with this phase, we present Figure 24. This figure shows the earthquakes having the pre-S phase at station PRB and station WMD. It is noteworthy that earthquakes under PRB are mostly responsible for observations of pre-S at WMD while earthquakes under WMD are mostly responsible for observations of pre-S under PRB, a sort of "reversed profile" on which the south end of HCF falls about midway between the two stations.

We have been proceeding with the working hypothesis that these pre-S phases are P reflections from shallow crustal anomalies (otherwise why would these phases have an appearance more like P than S on records which show obvious deficiency of high-frequency energy in the S-wave as compared with the P). It is tempting, therefore, to imagine that these are reflections from shallow-crustal magma bodies. However, we can point out one substantial problem with this idea. In their work on the Rio Grand rift of New Mexico, Sanford *et al.* (1973) presented reflections from what they take to be a possible zone of magma, but the reflected phase is clearly an S wave, not a P. In fact, S should reflect more strongly than P from a solid-liquid interface, so we would expect to find strong post-S reflections if the pre-S phases are reflected P, and these are almost nowhere seen. However, in the records presented by Sanford *et al.* (1973) we can see what looks like a pre-S reflection (although it is weaker than the post-S phase); moreover, the reflecting horizons there are assumed to be almost flat-lying, while at Mammoth such reflectors must have substantial dip, which may account for the relatively greater amplitudes for the pre-S phases at Mammoth.

2.3.4. Pre-S Phases North of the Caldera. Following the work of Zucca and Mills (1986) we have recently found another strong and unexpected phase at the single station SLK, to the NW of Long Valley caldera. An example of a record showing this phase is given in Figure 25; the earthquakes which produce this phase are given in Figure 26. In Figure 27 we present a travel time curve for the P-wave arrivals, S-wave arrivals, and the SLK phase. Note that the earthquakes which show the phase at SLK occur in a rather limited zone south of the caldera (compare Figures 26 and 7). The shape of this zone is a NW-trending ellipse pointed at the SLK station. Looking at Figure 25 we see that, unlike the pre-S

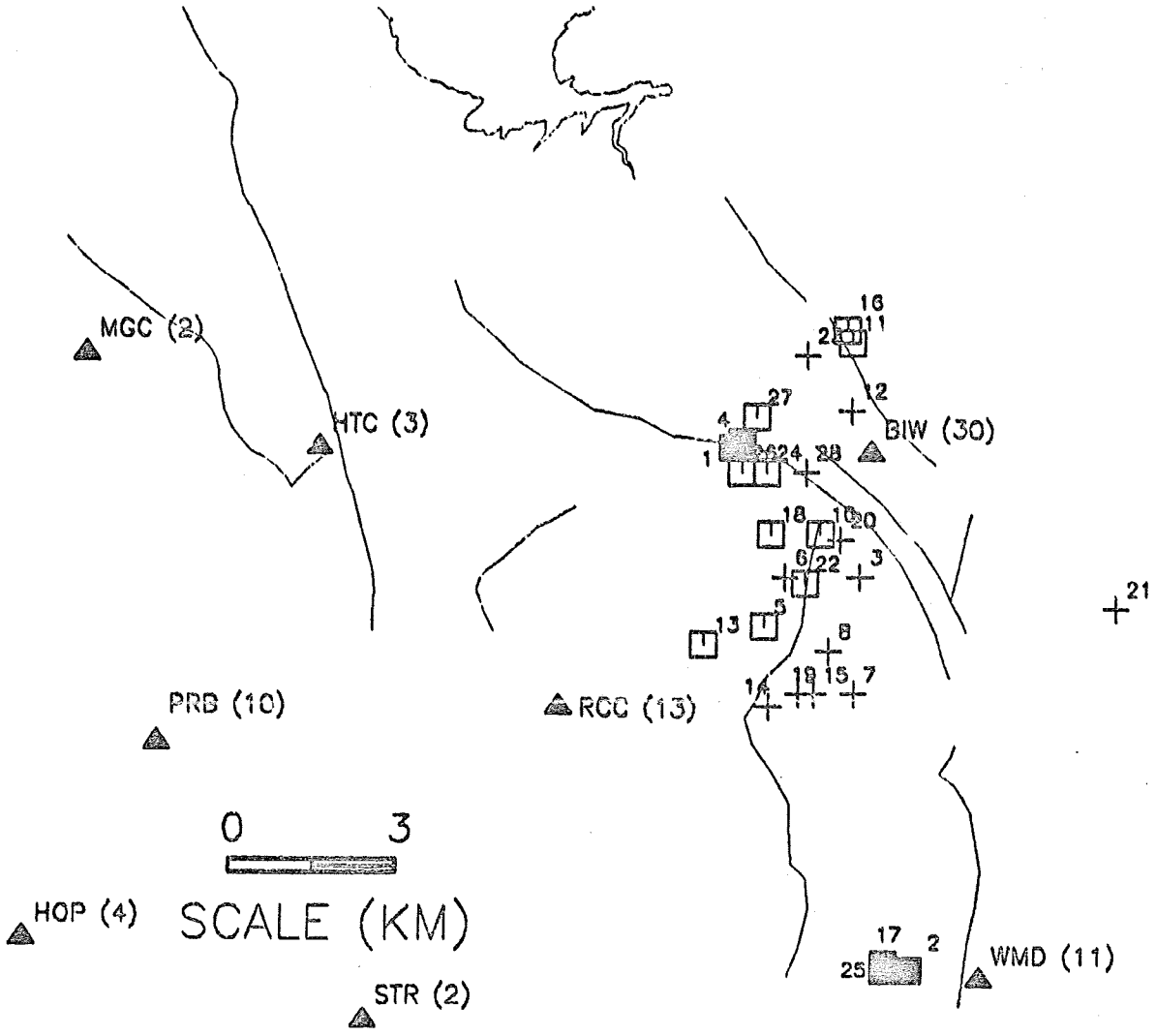

Figure 22. USGS locations of some of the aftershocks of the 04 October 1978 Wheeler Crest earthquake. *Closed symbols* denote earthquakes showing the pre-S reflection, with the solid symbols for those showing it strongly, and *open crosses* are earthquakes not showing the pre-S reflection at station BIW. Filled triangles are stations where the pre-S phase has been seen.

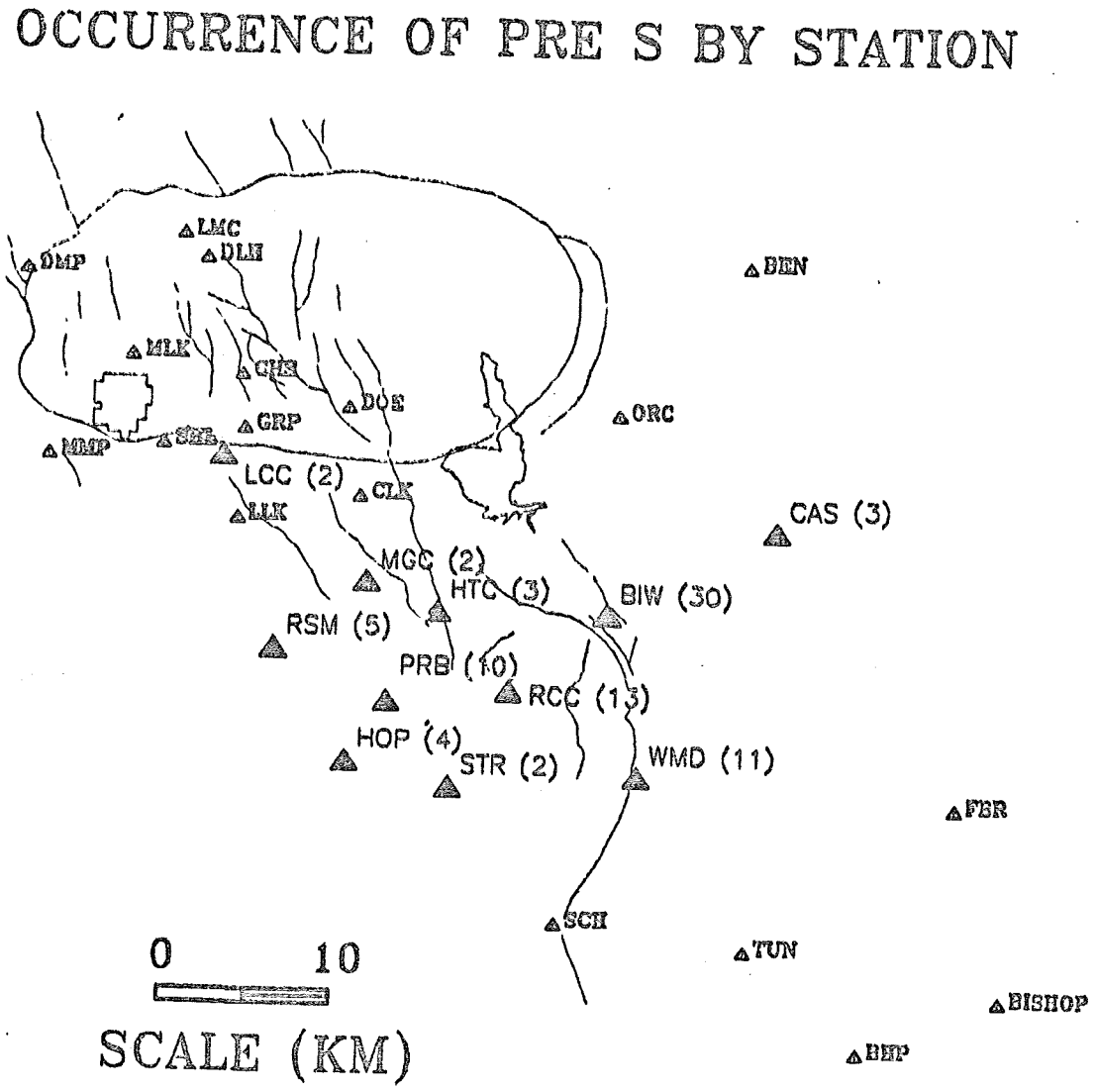

Figure 23. Occurrence of pre-S phases by station, with the numbers in parentheses giving the number of observations at that station. The stations in smaller letters are those for which 1 or fewer observation of pre-S has been seen. The south end of Hilton Creek fault is the line which ends by the letter B in PRB.

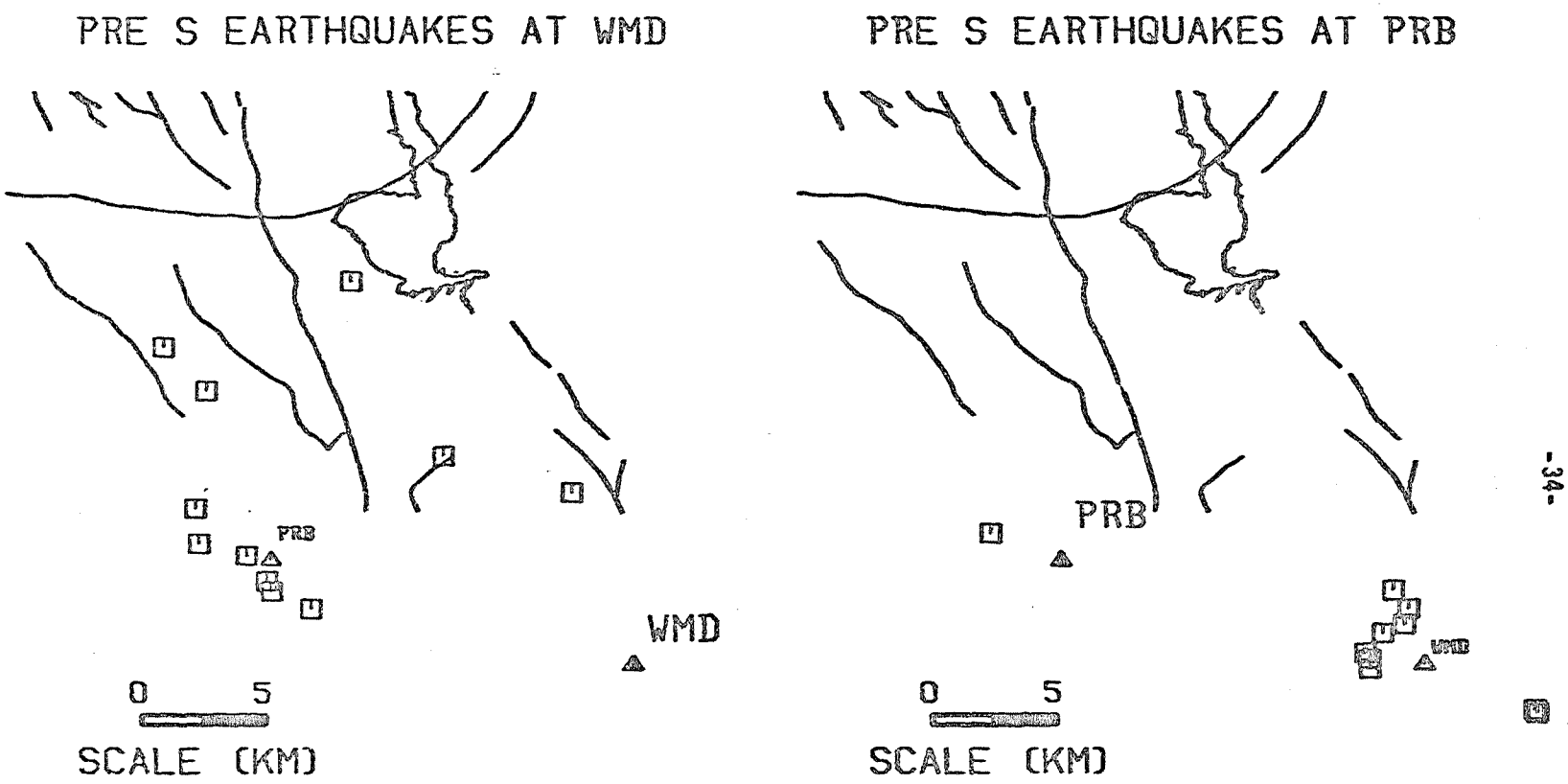

Figure 24. Occurrence of pre-S phases at stations PRB and WMD. Note that the south end of Hilton Creek fault lies between these two stations.

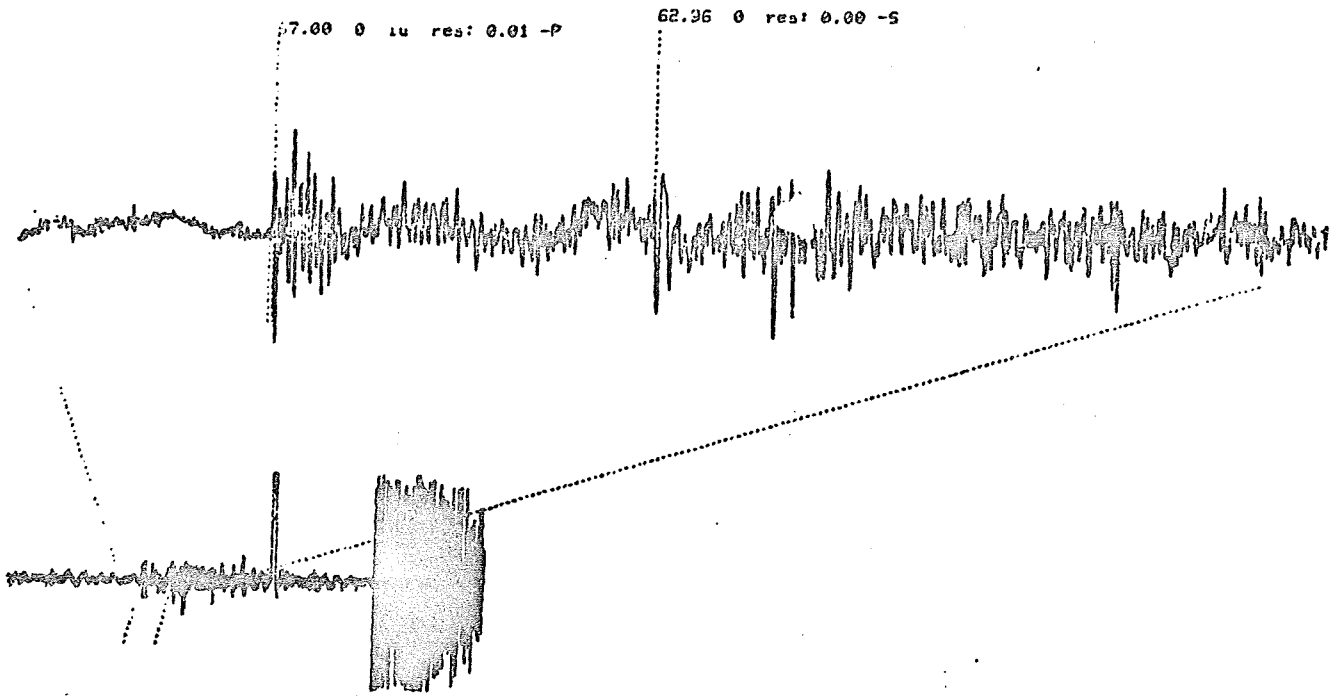

Figure 25. Example of a pre-S phase at station SLK for the earthquake of 26 November 1984 at 1627 GCT. The phase identified as "P" is the P arrival and the phase identified as "S" is the pre-S arrival (with true S following about one second later).

Pre–S Phases at Station SLK

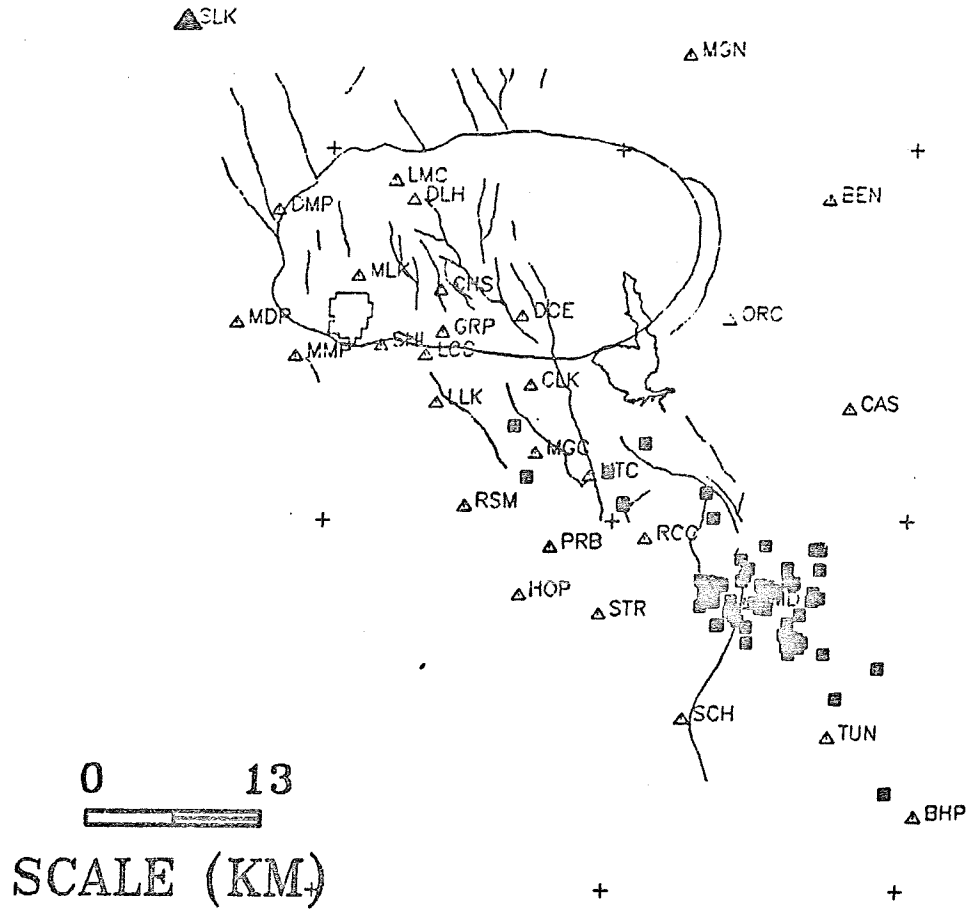

Figure 26. Station SLK (solid triangle upper left) and the earthquakes (solid squares) which have given rise to the pre-S phase at that station.

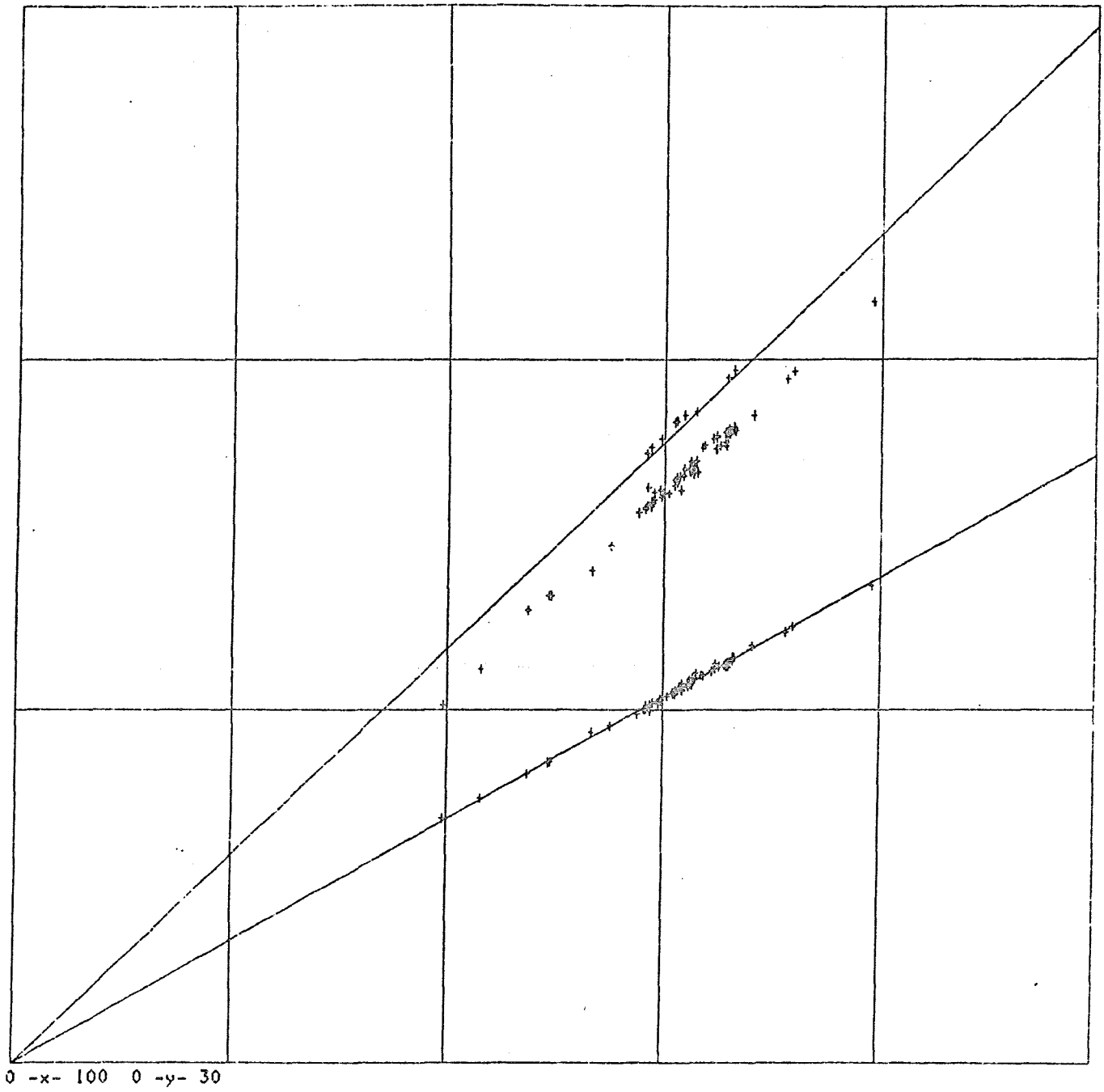

Figure 27. Travel time data for P, pre-S, and S arrivals at station SLK, with abscissas ranging from 0 to 100 km and ordinates ranging from 0 to 30 seconds. The two lines show predicted half space travel time curves (surface sources) for P and for S at velocities of 5.8 and 3.4 km/sec. The line of observations *preceding* those of S are the arrivals in question. Note that, over quite a range in distance, the pre-S travel time curve parallels S, and that the intercept of a line drawn through these data is negative.

phases that are seen south of the caldera, the character of the SLK phase is more like S than P. Figure 27 suggests that the phase is associated with S rather than P, because over quite a considerable distance range the travel-time curve appears to track that of the S phase. However, again we are faced with a problem of interpretation: note that the intercept time of the SLK phase is *negative*. It is impossible to obtain a travel time curve with negative intercept for any layer model in which the layers are flat lying (for flat-lying structures the slowness must be strictly non-increasing, and the intercept at close distances is zero).

It is not easy to conjure up models which come close to producing a travel time curve to match the observations shown in Figure 27, but one model is suggested. Noting that the earthquakes showing the SLK phase occur in a northwesterly trend, and that this trend passes close to the magma bodies proposed by Sanders (1984), we have hypothesized that the SLK phase is an S which converts to P in the magma body then back to an S for the remainder of the travel path to SLK. A crude and preliminary example of ray tracing, which gives approximately the right values for the travel times, is given in **Figure 28**. This hypothesis involves two S to P conversions at rather small angles of incidence. Therefore, on this hypothesis the amplitude of the SLK phase would be expected to be quite a bit smaller than the amplitude of S, an obvious problem since this phase is both quite strong and commonly observed.

We note in passing that, although the SLK phase appears to be similar in appearance to a similar pre-S phase seen by Zucca and Mills (1986) for an array near and east of SLK, the nature of his phase is quite different, showing a travel time with slowness markedly different from that of S (he hypothesizes that his pre-S phase is a deep P-reflection from the bottom of a magma body).

Task 3. Study of Magma Bodies.

In the previous section we have documented several independent lines of evidence which suggest the participation of shallow-crustal magma in the distortion of locally-recorded waveforms. While the method of S-wave shadowing, so successfully employed in the past, has been a disappointment in the analysis so far done using the digital on-line data, we continue to accumulate evidence for at least one major crustal anomaly in the mountain block *south* of the caldera. In particular, it now seems quite reasonable to pinpoint the map location of one of these as being located near the south end of Hilton Creek fault. The evidence for the association of magma with this spot, given in chronological order of discovery, is as follows: (1) focal mechanisms of the larger earthquakes of the Mammoth Lakes sequence, obtained from the inversion of body-wave teleseismograms, are suggestive of non double-couple focal mechanisms more typical of a dyke-injection type of source (Julian, 1983; Aki, 1984). Two of these earthquakes, those of 27 May 1980 and 04 October 1978, more or less straddle the south end of HCF; (2) S-wave shadowing has been documented by Ryall and Ryall (1984) for several areas south of the caldera (see Figure 12). The best documented case is the south end of HCF; (3) a very unusual post-S phase seen at Benton has particle motion which is that of a Rayleigh wave whose direction of approach is from the approximate direction of the south end of HCF (Figures 13 and 14); (4) strong pre-S phases, seen quite commonly at stations south of the caldera, show a decided concentration around the south end of HCF (Figure 23), with more direct evidence for its participation in the geometric disposition of epicenters and stations showing the phase (Figure 24). To this evidence, we can add a fifth point, which is documented in **Figure 29**. In this figure is shown a map of the better-quality epicenters as recorded by the on-line system since May 1984. Comparing with Figure 12, we see that two of the three shallow-

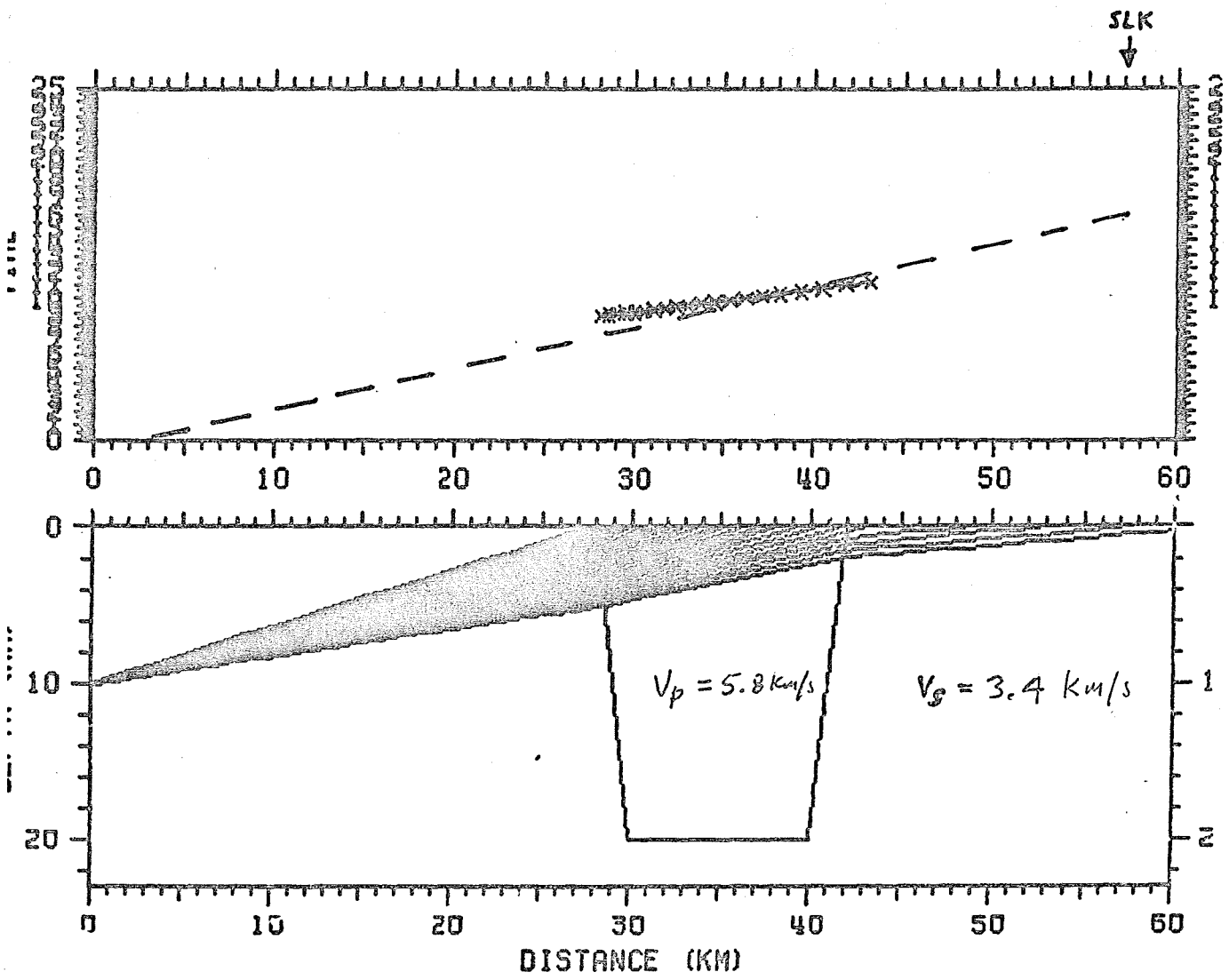

Figure 28. A crude, preliminary ray tracing model to show one way to obtain a pre-S arrival with a negative intercept time. If midway along the travel path the S converts to a P, and then back to an S, then the resulting travel time predicted is the dashed curve in the upper plot (with a negative intercept).

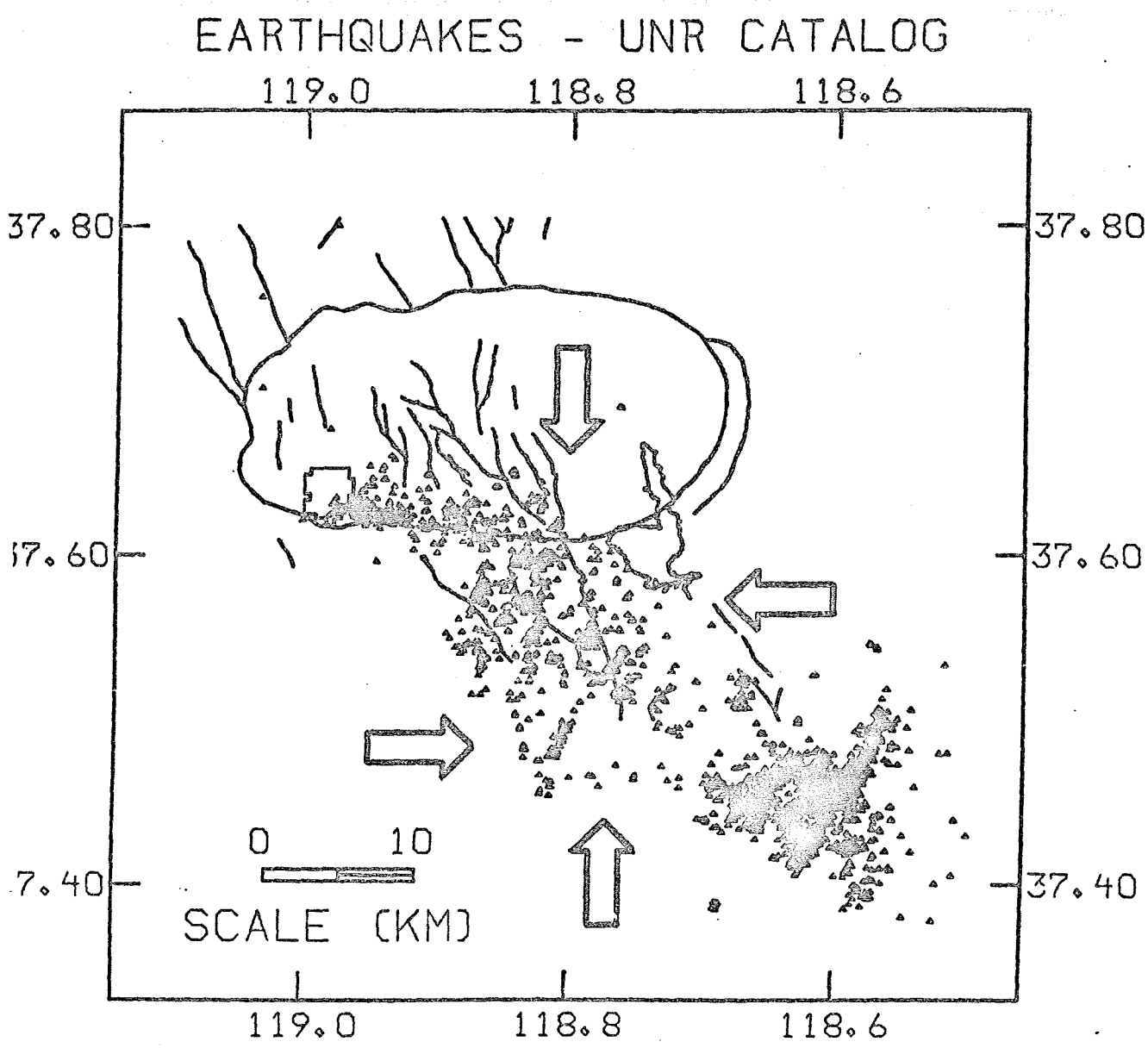

Figure 29. UNR catalog locations of earthquakes south of the caldera. The arrows point to two spots, midway along and at the south end of Hilton Creek fault, in which seismicity is absent. So far as we know, earthquakes are not known to occur in these regions at any time (including during the intense aftershock sequence in 1980). These spots are two zones of S-wave shadowing identified independently by Ryall and Ryall (1984): see Figure 12.

crustal zones of S-wave screening proposed by Ryall and Ryall (1984) are areas where earthquakes were absent within the seismically active zone south of Long Valley caldera. The largest of these is near the south end of HCF. All of this encourages us to proceed in our efforts at trying to refine and constrain the size and shape of a causative crustal anomaly (magma body?) near this location, and, as documented elsewhere in this report, the travel time and hypocenter information we have have provided the basis for our tentative description of this anomaly: we suppose that it is roughly cylindrical in shape, a few km in diameter, centered near the south end of Hilton Creek fault, and in the depth range 5 to 10 km. Such a model appears grossly in agreement with all of the observations we have noted so far.

The recent discovery of the SLK phase offers an excellent new opportunity to bring constraints to bear on the size and nature of the magma bodies within Long Valley caldera. If this really is an S to P to S conversion, then, because the velocity in the magma is relatively *high* compared with the direct travel path, the waves will search this anomaly out (rather than bypass it as a low velocity zone). This then provides the ability to time precisely the travel time of P through it and, therefore, if we can obtain good estimates for the velocity independently, on its geometry.

REFERENCES CITED

Aki, K., 1984. Evidence for magma intrusion during the Mammoth Lakes earthquakes of May 1980 and implications of the absence of volcanic (harmonic) tremor, *Jour. Geophys. Res.*, **89**, 7689-7696.

Bakun, W.H. and McEvilly, T.V., 1979. Recurrence models and Parkfield, California earthquakes, *Science*, **205**, 1375-1377.

Barker, J.S. and T.C. Wallace, 1985. Inversion of the teleseismic body waves for the moment tensor of the November 23, 1984 Round Valley, California earthquake, *EOS, Trans. Am. Geophys. Un.*, **66**, 952.

Bryant, W.A. (1984). Round Valley Fault Zone, Inyo and Mono Counties, *California Division of Mines and Geology, Fault Evaluation Report FER-158*, 6p.

Corbett, E.J. (1985). The Round Valley, California earthquake of November 23, 1984, *Earthquake Notes*, **56**, **no.1**, 30.

Corbett, E.J., D.M. Martinelli, and K.D. Smith (1985). Aftershock locations of the November 23, 1984 Round Valley, California earthquakes, *EOS, Trans. Amer. Geophys. Union*, submitted.

Lide, C.S., 1984. *Aftershocks of the May 1980 Mammoth Lakes, California, Earthquakes*, Univ. of Nevada M.S. Thesis.

Lide, C.S. and Ryall, A.S., 1985. Aftershocks of the May 1980 Mammoth Lakes, California, Earthquakes, *Interim Report on USDOE Contract DE-AS08-82ER12082 and USGS Contract 14-08-0001-21986, University of Nevada Seismological Laboratory Reno.*

Lide, C.S. and Ryall, A.S., 1985. Aftershock distribution related to the controversy regarding mechanisms of the May 1980, Mammoth Lakes, California, Earthquakes, *Jour. Geophys. Res.*, **90**, 11,151-11,154.

Hill, D.P. (1976). Structure of Long Valley caldera from a seismic refraction

experiment, *J. Geophys. Res.* **81**, 745-753.

Julian, B.R., 1983. Evidence for dyke intrusion earthquake mechanisms near Long Valley caldera, California, *Nature*, **303**, 323-325.

Julian, B.R. and Sipkin, S.A., 1985. Earthquake processes in the Long Valley caldera area, California, *Jour. Geophys. Res.*, **90**, 1,155-11,169.

Mayo, E.B., 1937. Sierra Nevada pluton and crustal movement, *Gour. Geol*, **45**, 169-192.

Nicks, W. F., Priestley, K.F. and Ryall, A.S., 1983. Nevada digital seismic network, *Earthquake Notes*, **54**, 15-16.

Peppin, W.A., 1985. New evidence for magma bodies south of Long Valley caldera, Mammoth Lakes, California, *EOS, Trans. Am. Geophys. Un.*, **66**, 959.

Pitt, A.M. and Steeples, D.W., 1975. Microearthquakes in the Mono Lake-northern Owens Valley, California region from September 28 to October 16, 1970, *Bull. Seism. Soc. Am.*, **65**, 835-844.

Rundle, J.B., and J.H. Whitcomb (1984). A model for deformation in Long Valley, California, 1980-1983, *J. Geophys. Res.* **89**, 9371-9380.

Rundle, J.B., and 21 others (1985). Seismic imaging in Long Valley, California by surface and borehole techniques: An investigation of active tectonics, *EOS, Trans. Am. Geophys. Union*, **66**, 194-201.

Ryall, A.S. and Hill, D.P., 1984. The Round Valley earthquake sequence, *unscheduled presentation at the Fall American Geophysical Union meeting*, 7 December 1984, San Francisco.

Ryall, F. and A. Ryall (1981). Attenuation of P and S waves in a magma chamber in Long Valley Caldera, California, *Geophys. Res. Lett.* **8**, 557-560.

Ryall, A. and F. Ryall (1983). Spasmodic tremor and possible magma injection in Long Valley caldera, eastern California, *Science*, **219**, 1432-1433.

Ryall, A. S. and F.D. Ryall, (1984). Shallow magma bodies related to lithospheric extension in the western Great Basin, western Nevada and eastern California, *Earthquake Notes*, **55**,11.

Sanders, C.O. (1984). Location and configuration of magma bodies beneath Long Valley, California determined from anomalous earthquake signals, *J. Geophys. Res.*, in press.

Sanders, C.O. and F. Ryall (1983). Geometry of magma bodies beneath Long Valley, California determined from anomalous earthquake signals, *Geophys. Res. Letters* **10**, 690-692.

Sanford, A.R., Alptekin, O. and T.R. Toppozada (1973). Use of reflection phases on microearthquake seismograms to map an unusual discontinuity beneath the Rio Grande rift, *Bull. Seism. Soc. Am.*, **63**, 2021-2034.

Savage, J.C. and M.M. Clark (1982). Magmatic resurgence in the Long Valley Caldera, California: Possible cause of the 1980 Mammoth Lakes earthquakes, *Science* **217**, 531-533.

Smith, K.D., D.M. Martinelli, and E.J. Corbett (1985). Focal mechanisms of the November 23, 1984 Round Valley, California earthquakes, *EOS, Trans. Amer. Geophys. Union*, submitted.

Somerville, M.R. and Peppin, W.A. (1979). Recent seismicity patterns near Mammoth Lakes, California, *Earthquake Notes, Seism Soc. Am.*, **50**, 4.

Somerville, M.R. and Peppin, W.A. (1980). Mammoth Lakes-Bishop seismicity, past and present, *EOS, Trans. Am. Geophys. Un.*, **61**, 1041.

Vetter, U.R., 1986. Focal mechanisms and the western boundary of the Great Basin tectonic province, *abstract submitted to the Seismological Society of America*, spring meeting at Charleston, SC.

Zucca, J.J. and Mills, J.M., 1986. Observation of a reflection from the base of a magma chamber in Long Valley caldera, California, *Bull. Seism. Soc. Am.*, submitted.

PUBLICATIONS, ABSTRACTS, AND PENDING RESEARCH PROJECTS

In this section we present a list of published works, abstracts, and a summary of research in progress (for which DOE will receive acknowledgment).

Publications.

Hill, D.P., Bailey, R.A., and Ryall, A.S., 1985. Active Tectonic and Magmatic processes beneath Long Valley caldera, Eastern California: An Overview, *Jour. Geophys. Res.* **90**, 11,111-11,120.

Lide, C.S., 1984. *Aftershocks of the May 1980 Mammoth Lakes, California, Earthquakes*, Univ. of Nevada, M.S. Thesis., 78p.

Lide, C.S. and Ryall, A.S., 1985. Aftershocks of the May 1980 Mammoth Lakes, California, Earthquakes, *Interim Report on USDOE Contract DE-AS08-82ER12062 and USGS Contract 14-08-0001-21986*, University of Nevada Seismological Laboratory, Reno, 82p.

Lide, C.S. and Ryall, A.S., 1985. Aftershock distribution related to the controversy regarding mechanisms of the May 1980, Mammoth Lakes, California, Earthquakes, *Jour. Geophys. Res.*, **90**, 11,151-11,154.

Ryall, A.S. and Ryall, F.D., 1983. Spasmodic tremor and possible magma injection in Long Valley caldera, eastern California, *Science*, **219**, 1432-1433.

Sanders, C.O., 1984. Location and configuration of magma bodies beneath Long Valley, California determined from anomalous earthquake signals, *Jour. Geophys. Res.*, **89**, 8287-8302.

Sanders, C.O. and Ryall, F.D., 1983. Geometry of magma bodies beneath Long Valley, California determined from anomalous earthquake signals, *Geophys. Res. Letters*, **10**, 690-692.

Vetter, U.R., Ryall, A.S., and Sanders, C.O., 1983. Seismological investigations of volcanic and tectonic processes in the western Great Basin, Nevada and eastern California, *Geothermal Resources Council, Special Rpt. 13*, 333-343.

Vetter, U.R., 1984. Focal mechanisms and crustal stress patterns in western Nevada and eastern California, *Annales Geophysicae*, 699-710.

Vetter, Ute R., 1984. Focal mechanisms and frequency-depth distribution of earthquakes in the Mammoth Lakes area, *Active Tectonic and Magmatic Processes beneath Long Valley Caldera, eastern California, U.S. Geol. Survey Open-File Rpt. 84-939*, 453-481.

Vetter, Ute and Ryall, A.S., 1983. Systematic change of focal mechanism with depth in the western Great Basin, *Jour. Geophys. Res.*, **88**, 8237-8250.

Vetter, U.R., and Smith, G.D., 1985. Bulletin of the Seismological Laboratory for the period January 1 to December 31, 1981, *Univ. of Nevada report*, 34p.

Abstracts.

Corbett, E.J., 1985. The Round Valley, California earthquake of November 23, 1984, *Earthquake Notes*, 56, 30.

Corbett, E.J., Martinelli, D.M. and Smith, K.D., 1985. Aftershock locations of the November 23, 1984 Round Valley, California earthquake, *EOS, Trans. Am. Geophys. Un.*, 46, 952.

Peppin, W.A., 1985. New evidence for magma bodies south of Long Valley caldera, Mammoth Lakes, California, *EOS, Trans. Am. Geophys. Un.*, 46, 959.

Peppin, W.A. and Honjas, W., 1986. Further evidence on the crustal anomaly (magma body?) near the south end of Hilton Creek fault, Mammoth Lakes, California, *abstract submitted to the Seismological Society of America*, Charleston, SC.

Ryall, A.S. and Hill, D.P., 1984. The Round Valley earthquake sequence, *unscheduled presentation at the Fall American Geophysical Union meeting, 7 December, San Francisco.*

Ryall, A.S. and Ryall, F.D., 1984. Shallow magma bodies related to lithospheric extension in the western Great Basin, western Nevada and eastern California, *Earthquake Notes*, 55, 11.

Smith, K.D., Martinelli, D.M. and Corbett, E.J., 1985. Focal mechanisms of the November 23, 1984 Round Valley, California earthquakes, *EOS, Trans. Am. Geophys. Un.*, 46, 952.

Vetter, U.R., 1984. Earthquake frequency, focal mechanisms, and temperature in the western Great Basin-Mammoth Lakes Region, Nevada and eastern California. *EOS, Trans. Am. Geophys. Union*, 65, 1118.

Vetter, U.R., 1986. Focal mechanisms and the western boundary of the Great Basin tectonic province, *abstract submitted to the Seismological Society of America*, Charleston, SC.

Manuscripts in Preparation.

Corbett, E.J., Martinelli, D.M. and Smith, K.D., 1986. Aftershock locations of the November 23, 1984 Round Valley, California earthquake, *Bull. Seism. Soc. Amer.*, in preparation.

Peppin, W.A., 1986. The observations of remarkable seismic phases recorded locally for earthquakes in the vicinity of Long Valley caldera, California.

Peppin, W.A., 1986. A shallow-crustal anomaly (magma body?) near the south end of Hilton Creek fault, California. 1. Description based on the observations of several hundred anomalous seismic phases.

Attachments

Reprints removed.
DSW

ABSTRACT

This report summarizes efforts made by the Seismological Laboratory toward the detection and delineation of shallow crustal zones in the western Great Basin, and toward the development of methods to accomplish such detection. The work centers around the recently-active volcanic center near Long Valley, California. The work effort is broken down into three tasks: (1) network operations, (2) data analysis and interpretation, and (3) the study of shallow crustal anomalies (magma bodies). Section (1) describes the efforts made to record thousands of earthquakes near the Long Valley caldera, and focusses on the results obtained for the November 1984 Round Valley earthquake. Section (2) describes the major effort of this contract, which was to quantify the large volume of seismic data being recorded as it pertains to the goals of this contract. Efforts described herein include (i) analysis of earthquake focal mechanisms, and (ii) the classification, categorization, and interpretation of unusual seismic phases in terms of reflections and refractions from shallow-crustal anomalous zones. Section (3) summarizes the status of our research to date on the locations of magma bodies, with particular emphasis on a location corresponding to the map location of the south end of Hilton Creek fault. Five lines of independent evidence, suggest that magma might be associated with this spot. Finally, new evidence on the large magma bodies within the Long Valley caldera, of interest to the DOE deep drilling project, is presented.

END

DATE FILMED

06/09/86